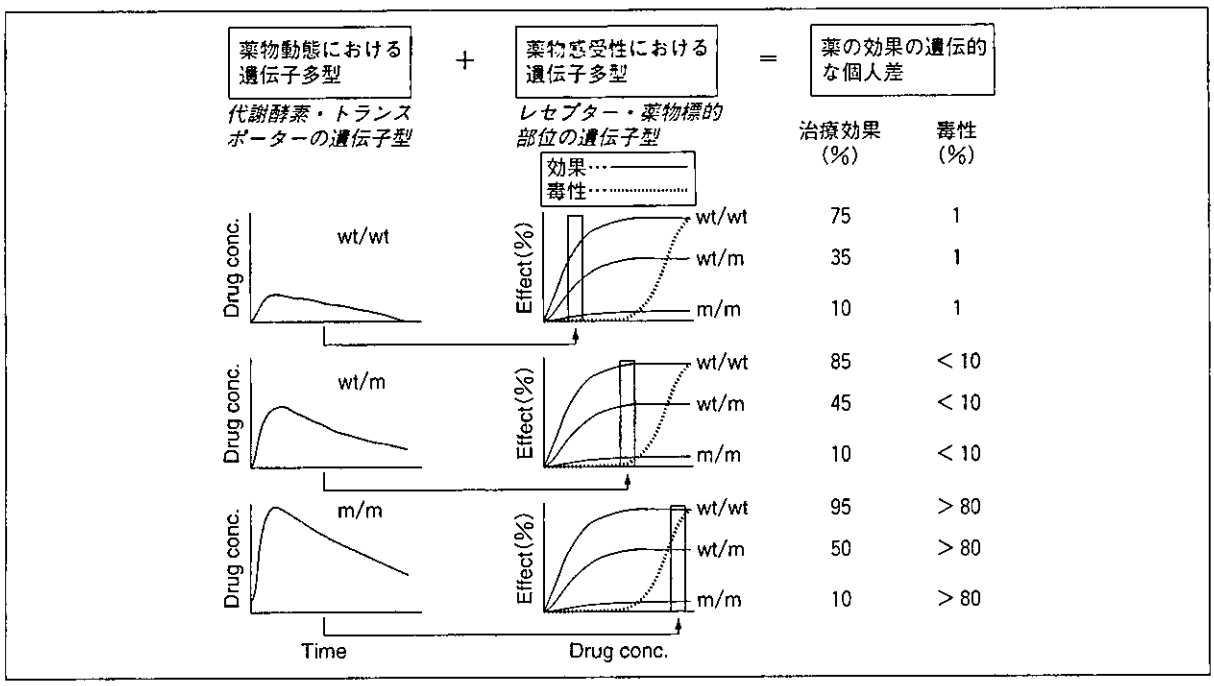

図1　薬物動態関連因子・薬効標的分子の遺伝子型と，治療効果・毒性発現の関係
（文献35より引用，改変）

ターであれば細胞への取り込みあるいは排泄が遅延することによる血中濃度や組織中濃度の変動が予想できる．特に，薬物代謝・輸送においてもっぱら1種類の蛋白により変換・輸送される薬物，もしくは複数の代謝・輸送経路のなかで特に寄与率の高い経路がある薬物の場合，そのような経路に関わる蛋白の遺伝子多型による影響は特に大きいと思われる．

現在はまだ，遺伝子診断により，あらゆる薬物に対する応答性が予見できるという段階までは達しておらず，各々の酵素やトランスポーターが薬物動態に与える影響の解明とともに，SNPs (single nucleotide polymorphism)などに起因する変異蛋白の機能変動の解析から，臨床上意味のあるSNPsが探索されている段階である．これら情報の集積に伴い，あらかじめ，薬効の個人差を引き起こすと思われる遺伝子の多型診断の結果に基づく層別化臨床試験の実施や，遺伝子型に基づく処方設計により血中濃度や薬効の個人差を生み出す要因をできる限り減らした薬物治療などが今後の課題となる．特に，抗がん剤においては，治療域と中毒域が接近しているため，小さな個人間変動でも，致死的な毒性や予測外の効果が発現しうる．本稿では，薬物動態関連因子の遺伝子多型について概説したい．

抗がん剤の薬物動態に関わる遺伝子多型

薬物の血中濃度は，標的臓器やクリアランス臓器への薬物トランスポーターなどを介した輸送，代謝による活性化・不活化などの様々な因子により決定されている．そのなかで，現在までに臨床的に注目されてきた遺伝子多型の例としては，チトクロームP450を中心とした代謝酵素によるものが挙げられる，これに関しては，本特集別項を参照されたい．ここではその他の抱合・代謝酵素ならびにトランスポーターにおいて，今までに個人差の報告があった薬剤とその原因となる遺伝子多型について表1にまとめる．以下に，具体例を挙げて概説する．

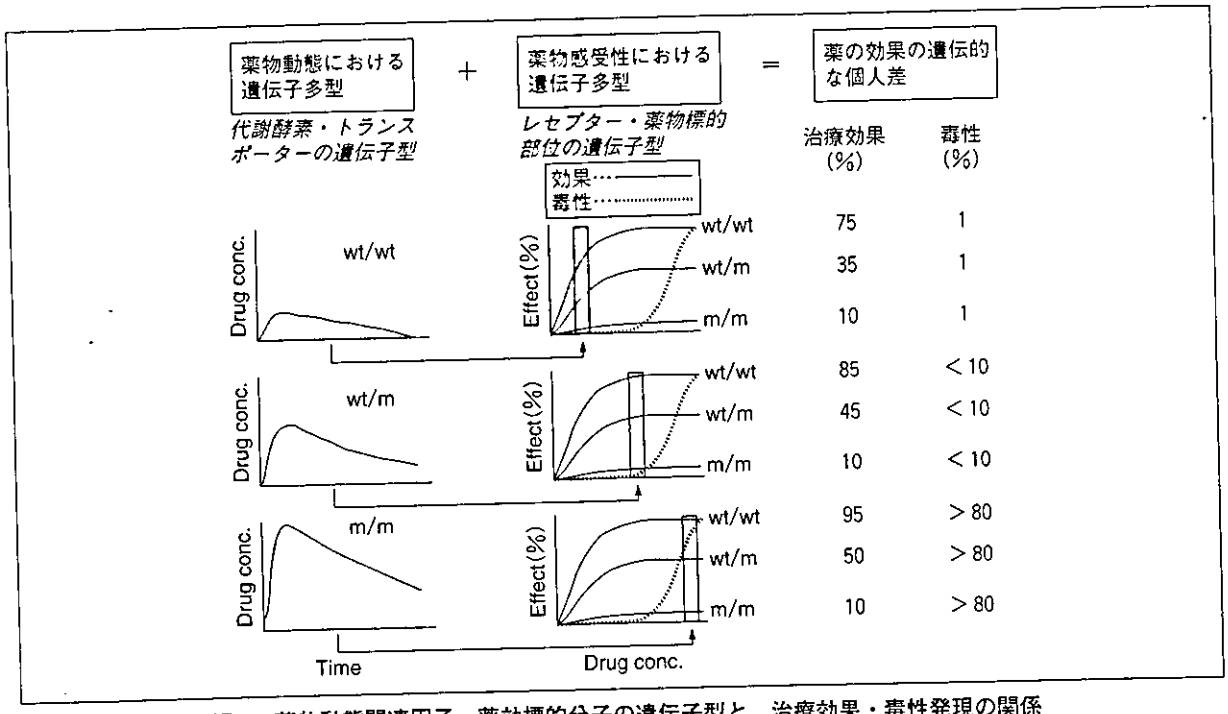

図1　薬物動態関連因子・薬効標的分子の遺伝子型と，治療効果・毒性発現の関係
（文献35より引用，改変）

ターであれば細胞への取り込みあるいは排泄が遅延することによる血中濃度や組織中濃度の変動が予想できる．特に，薬物代謝・輸送においてもっぱら1種類の蛋白により変換・輸送される薬物，もしくは複数の代謝・輸送経路のなかで特に寄与率の高い経路がある薬物の場合，そのような経路に関わる蛋白の遺伝子多型による影響は特に大きいと思われる．

現在はまだ，遺伝子診断により，あらゆる薬物に対する応答性が予見できるという段階までは達しておらず，各々の酵素やトランスポーターが薬物動態に与える影響の解明とともに，SNPs (single nucleotide polymorphism)などに起因する変異蛋白の機能変動の解析から，臨床上意味のあるSNPsが探索されている段階である．これら情報の集積に伴い，あらかじめ，薬効の個人差を引き起こすと思われる遺伝子の多型診断の結果に基づく層別化臨床試験の実施や，遺伝子型に基づく処方設計により血中濃度や薬効の個人差を生み出す要因をできる限り減らした薬物治療などが今後の課題となる．特に，抗がん剤においては，治療域と中毒域が接近しているため，小さな個人間変動でも，致死的な毒性や予測外の効果が発現しうる．本稿では，薬物動態関連因子の遺伝子多型について概説したい．

抗がん剤の薬物動態に関わる遺伝子多型

薬物の血中濃度は，標的臓器やクリアランス臓器への薬物トランスポーターなどを介した輸送，代謝による活性化・不活化などの様々な因子により決定されている．そのなかで，現在までに臨床的に注目されてきた遺伝子多型の例としては，チトクロームP450を中心とした代謝酵素によるものが挙げられる，これに関しては，本特集別項を参照されたい．ここではその他の抱合・代謝酵素ならびにトランスポーターにおいて，今までに個人差の報告があった薬剤とその原因となる遺伝子多型について表1にまとめる．以下に，具体例を挙げて概説する．

表1　薬物代謝・抱合酵素，トランスポーターの遺伝子多型の例

薬　剤	代謝・抱合酵素，トランスポーター	遺伝子	多型の種類
Amonafide	N-acetyltransferase	*NAT2*	*NAT2*5*, *NAT2*6A*, *NAT2*7*, *NAT2*13*, *NAT2*14*
5-FU	DPD	*DPYD*	*DPYD*2A*
Mercaptopurine Azathiopurine	TPMT	*TPMT*	*TPMT*2*, *TPMT*3A*, *TPMT*3C*
CPT-11	UDP-glucuronosyltransferase	*UGT1A1*	*UGT1A1*28*
CMF regimen *1 葉酸拮抗剤	MTHFR *2	*MTHFR*	C 677 T
Digoxin, fexofenadine *3	MDR 1	*MDR1*	C 3435 T, G 2677 (T,A)
Pravastatin	OATP-C	*OATP-C*	*OATP-C*15*

*1 CMF：cyclophosphamide, methotrexate, 5-FU　*2 MTHFR：methylenetetrahydrofolate reductase
*3 詳細は文献37を参照されたい．

（文献36の表に追加，改変）

TPMT（thiopurine methyltransferase）

プリン代謝拮抗薬である6-メルカプトプリン(6-mercaptopurine)や，そのプロドラッグであるアザチオプリン(azathiopurine)は小児急性白血病やクローン病の治療に用いられ，体内でhypoxanthine phosphoribosyl transferase（HPRT)により6-thioguanine nucleotide (6-TGN)に変換され活性を示す一方，TPMTによりS-メチル化され，不活化されることが知られている．これまでに，TPMT活性と細胞内6-TGN濃度に相関がみられ，TPMTの活性低下による結果として生じる活性体(6-TGN)の産生上昇が代謝拮抗作用の増強，骨髄抑制などの副作用を呈することが報告されている[1)-3)]．このことから，TPMTの活性は，活性体(6-TGN)の血中濃度の調節にとって重要な要因であるといえる．TPMT活性には個人差が存在し，白人においては，約90％が高い活性，0.3％が低い活性，約10％がこれらの中間の活性を示す[4)]．この個人間の差を説明すべく遺伝子多型の解析が行われている．これまでの研究から，*TPMT*2*(Ala 80 Pro)，*TPMT*3A*(Ala 154 Thr)，*TPMT*3C*（Tyr 240 Cys）の遺伝子型により低TPMT活性の80～95％程度を説明しうると考えられている[1)5)]．これら変異蛋白においては，蛋白分解速度が上昇しており，その結果，働きうるTPMT量の減少と結びついていると考えられる[6)-8)]．現在では，PCRを用い，簡便に遺伝子型の診断をすることが可能であり[9)]，初期投与量のより安全な設定に繋がっていくものと推定される．

DPD（dehydropyrimidine dehydrogenase）

5-フルオロウラシル(5-fluorouracil；5-FU)は胃癌，結腸・直腸癌をはじめとする固形癌に適用される代謝拮抗型の抗癌剤であり，投与量のほとんどが，DPDにより不活性化されることが知られている．ソリブジンとの併用による5-FUの致死的な副作用も，ソリブジンの腸内細菌代謝物であるブロモビニルベンゼンによるDPDの非可逆的な不活性化から起こったことを鑑みても，DPDは5-FU代謝における重要な律速酵素であると考えられる[9)]．DPDには少なくとも20種類以上の遺伝子多型が報告されており，そのなかでも，*DPYD*2A*においては，スプライシング部位を決定するexon-intronジャンクション(GT)のGからAの変異によりexon 14の脱落が起こり，結果として本来翻訳されるべき55ア

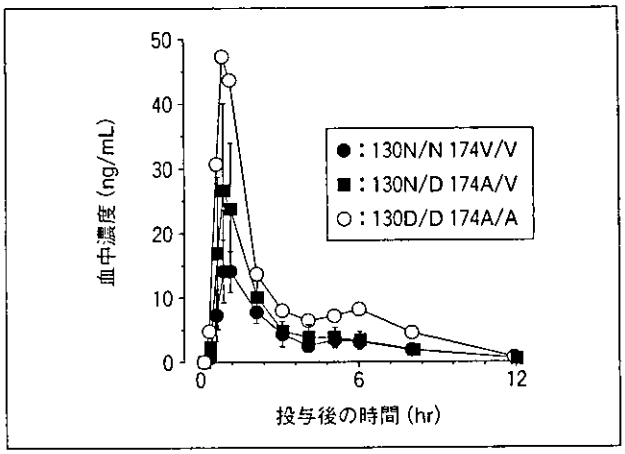

図2　*OATP-C* 遺伝子多型とプラバスタチン血中濃度推移
(文献34より引用、改変)

Dubin-Johnson 症候群の原因ともなる．また一方，極めて広範なアニオン性化合物や種々のグルタチオンやグルクロナイド抱合体を基質とし，塩酸イリノテカン(CPT-11)の活性代謝物である SN-38 やそのグルクロン酸抱合体である SN-38-Glu をはじめとした薬物の肝臓から胆汁中への排泄にも関与している[28)29)]．CPT-11 の副作用には，重篤な消化管障害があり，この発現には個人差が認められる．副作用の発現要因としては消化管内での SN-38 の曝露が挙げられ，その抱合や排泄に関与する一連の経路の遺伝子多型は重要であろうと思われる．現時点では，SN-38-Glu の生成に関わるグルクロン酸転位酵素(UDP-glucuronosyltransferase ； UGT)である UGT 1 A 1 の遺伝子多型の影響が最もよく研究されており，プロモーター領域に存在する TA リピートの回数が野生型と比べ 1 回多い *UGT1A1*28* における SN-38-Glu の生成の遅延や，強い副作用発現が観察されている[30)31)]．詳細に関しては，本特集別項を参照されたい．また，MRP 2 を介した SN-38 の胆汁排泄を阻害することで消化管毒性が軽減された報告や[32)]，SN-38 のヒト肝臓 canalicular membrane vesicles (CMVs)における輸送活性に顕著な個人差がみられていることから MRP 2 の遺伝子多型が副作用の個人差に関与している可能性も示唆され，今後の研究が待たれる[28)]．また，取り込みトランスポーターのうち，肝臓特異的に発現する OATP-C (OATP 2/SLC 21 A 6/LST-1)は，MRP 2 と類似の広範な基質認識性を有しており，メトトレキサート(methotrexate)なども基質とする[33)]．最近，HMG-CoA 還元酵素阻害剤であるプラバスタチン(pravastatin)の腎外クリアランスが *OATP-C*15* (Asn 130 Asp，Val 174 Ala)のアレルを持つ人において有意に低下するなど，トランスポーターの遺伝子多型が実際に臨床での薬物動態に影響を及ぼしていることが報告された(図 2)[34)]．一般に，トランスポーターの多くは広い基質認識性を持ち，抗癌剤もその例にもれない．したがって，抗癌剤の体内動態に関しても大きな影響を及ぼす可能性があり，今後の検討が必要とされる．

おわりに

以上，抗癌剤の薬物動態の個人間変動の原因となる遺伝子多型の例を取り上げた．これらの例は，実際の遺伝子多型と薬物動態によい相関がみられた例であるが，実際には，薬物の体内動態の責任因子が明らかになるにつれ，多くの例がこの先加わっていくものと思われる．また，これまでは単独の SNP のみが機能変動に関与する事例研究が主体であったが，前述の MDR 1 の例のように複数の SNPs を同時に持つことにより新たな機能変動に繋がる可能性もある．そのようなハプロタイプの形成を考慮した，*in vitro*，*in vivo* の両方向からの解析を進める重要性や，複数の蛋白における遺伝子多型の影響を統合的かつ定量的に判断し，臨床での予測に直接繋げる重要性が近年明らかになりつつある．これらの情報の集積に伴い，薬物ごとに，対象とすべき遺伝子多型の同定とその簡便な診断方法，複数の多型や他の要因を定量的にモデル化して合理的に投与量を判断する方法論の確立が必要となってくるであろうと考えている．

文　献

1) Otterness D, Szumlanski C, O'Brien J Weinshilboum R, et al ： Human thiopurine methyltransferase pharmacogenetics ： gene sequence polymorphisms. *Clin Pharmacol Ther* 62 ： 60-73, 1997
2) Yates CR, Krynetski EY, Evans WE, et al ： Molecular

ミノ酸が欠損した不完全な蛋白が発現することが知られている[10][11]．この蛋白においてはDPD活性が完全に欠損しており，*DPYD*2A* アレルを持つ患者が，5-FU投与により，重篤あるいは致死的な副作用を示した例が臨床的にも報告されている[12][13]．しかしながら，DPDの変異のみでは，5-FUの副作用発現を完全に予測することはできないこともわかっている．例えば，5-FU活性代謝物である5-fluoro-2-deoxyuridine monophosphate (5 FdUMP)の作用部位であるthymidylate synthase (TS)にも5'-promoter領域に28-bpの繰り返し配列の回数が異なる遺伝子多型が存在し，繰り返しが3回のhomozygoteにおいては，高いTSの発現量を示す結果，進行性大腸癌におけるdisease-free survival (DFS)の有意な低下が起こることが報告されている[14]．このようなケースでは，薬物動態(pharmacokinetics)関連因子のみならず，薬の作用する標的部位(pharmacodynamics)の面の両方の要因を考慮する必要がある．

トランスポーター

近年，様々なトランスポーターが，肝臓や腎臓といった薬物のクリアランス臓器や，脳など薬の効果・副作用に重要な影響を及ぼす臓器に発現し，様々な薬物や生体内物質の血液から細胞内への取込みや排泄に関与することにより，これら基質化合物の血中や標的臓器における濃度推移に影響を及ぼしていることが明らかとなってきた．

有機アニオン系薬物においては，主に，血中から臓器への取り込み過程に関与するorganic anion transporting polypeptide (OATP) family，organic anion transporter (OAT) familyや，細胞外への排出に関わるABCトランスポーターなどの同定が進んできた．しかし，これらトランスポーターの遺伝子多型が薬物動態に与える影響については，代謝酵素と比べ未解明な部分が多く残されている．MDR 1/P-glycoprotein (P-gp)は，広範な中性，塩基性薬物を認識し，塩酸イリノテカンやビンカアルカロイド類などの数多くの抗癌剤も基質とする[15][16]．これまで，MDR 1について多くの遺伝子多型が同定されているが，なかでも興味深いのは，アミノ酸変異を伴わないsilent mutation (C 3435 T)である．これは日本人においてアレル頻度が実に49.0％と高頻度に発現するSNPであり[17]，この変異を有する被験者について，消化管でのMDR 1の発現量の減少がみられ，おそらく管腔側における排出能力の低下に伴う吸収率の上昇により，基質薬物であるdigoxinが経口投与後，変異保有者において有意に高い血中濃度推移を示すことが報告されている[18]．しかしながら別の報告では，逆に血中濃度の低下を示すMDR 1の機能亢進を示唆する知見[19][20]もあり，一致した見解が得られていない．それに加え，C 3435 Tとアミノ酸の変異を伴うG 2677 (T,A)，silent mutationであるC 1236 Tの3つの変異間には高頻度のリンクがみられている[21][22]．このように複数のSNPsを同時に持つ場合に単独のSNPでは観察できなかった何らかの機能・発現変化が生まれる可能性，いわゆるハプロタイプを考慮し，層別化を行った臨床試験が行われつつある[22]-[26]．しかし，*MDR1* 遺伝子においては，ほぼすべての被験者において，最低1つの変異が観察される程，変異自体の存在が珍しくなく，またこれらSNP間で連鎖不平衡(Linkage Disequilibrium ； LD)が観察されており[22]，人種間でもハプロタイプ形成の頻度に大きな差がみられることから[21]，すべてのハプロタイプに対し統計的にデータの有意差を検出できる母集団を確保できるような臨床試験を行うのは非常に困難である．一方，*in vitro* 解析においては，C 3435 T，G 2677 (T,A)のSNPsを考慮したすべてのハプロタイプで，MDR 1の機能に変化が生じないことがLLC-PK 1細胞発現系を用いた実験ですでに示されている[27]．また，連鎖不平衡(LD) blockの統計的解析により，上記の代表的な3変異の連鎖率からゲノム上でこれらにリンクする未知の変異が周囲40-80 kb以内に存在する可能性も示唆されており[21]，今後，このような *in vitro* 解析や，さらなる臨床試験による情報の蓄積が期待され，ハプロタイプ形成とMDR 1機能の相関が明らかとなっていくだろう．

また同じABCトランスポーターに属するMRP 2 (multidrug resistance-associated protein 2/ABCC 2)は抱合型ビリルビンなど内因性化合物を基質とし，その遺伝的変異に伴う機能喪失は，黄疸を主症状とする

diagnosis of thiopurine S-methyltransferase deficiency : genetic basis for azathioprine and mercaptopurine intolerance. *Ann Intern Med* **126** : 608-614, 1997
3) McLeod HL, Krynetski EY, Evans WE, et al : Genetic polymorphism of thiopurine methyltransferase and its clinical relevance for childhood acute lymphoblastic leukemia. *Leukemia* **14** : 567-572, 2000
4) Weinshilboum RM, Sladek SL : Mercaptopurine pharmacogenetics : monogenic inheritance of erythrocyte thiopurine methyltransferase activity. *Am J Hum Genet* **32** : 651-662, 1980
5) Tai HL, Krynetski EY, Evans WE, et al : Thiopurine S-methyltransferase deficiency : two nucleotide transitions define the most prevalent mutant allele associated with loss of catalytic activity in Caucasians. *Am J Hum Genet* **58** : 694-702, 1996
6) Tai HL, Krynetski EY, Y Evans WE, et al : Enhanced proteolysis of thiopurine S-methyltransferase (TPMT) encoded by mutant alleles in humans (TPMT•3 A, TPMT•2) : mechanisms for the genetic polymorphism of TPMT activity. *Proc Natl Acad Sci U S A* **94** : 6444-6449, 1997
7) Krynetski EY, Schuetz JD, Evans WE, et al : A single point mutation leading to loss of catalytic activity in human thiopurine S-methyltransferase. *Proc Natl Acad Sci U S A* **92** : 949-953, 1995
8) Tai HL, Fessing MY, Evans WE, et al : Enhanced proteasomal degradation of mutant human thiopurine S-methyltransferase (TPMT) in mammalian cells: mechanism for TPMT protein deficiency inherited by TPMT•2, TPMT•3 A, TPMT•3 B or TPMT•3 C. *Pharmacogenetics* **9** : 641-650, 1999
9) Okuda H, Nishiyama T, Watabe T, et al : Lethal drug interactions of sorivudine, a new antiviral drug, with oral 5-fluorouracil prodrugs. *Drug Metab Dispos* **25** : 270-273, 1997
10) Meinsma R, Fernandez-Salguero P, Gonzalez FJ, et al : Human polymorphism in drug metabolism : mutation in the dihydropyrimidine dehydrogenase gene results in exon skipping and thymine uracilurea. *DNA Cell Biol* **14** : 1-6, 1995
11) Van Kuilenburg AB, Vreken P, Van Gennip AH, et al : Genotype and phenotype in patients with dihydropyrimidine dehydrogenase deficiency. *Hum Genet* **104** : 1-9, 1999
12) Raida M, Schwabe W, Hoffken K, et al : Prevalence of a common point mutation in the dihydropyrimidine dehydrogenase (DPD) gene within the 5'-splice donor site of intron 14 in patients with severe 5-fluorouracil (5-FU)-related toxicity compared with controls. *Clin Cancer Res* **7** : 2832-2839, 2001
13) van Kuilenburg AB, Muller EW, van Gennip AH, et al : Lethal outcome of a patient with a complete dihydropyrimidine dehydrogenase (DPD) deficiency after administration of 5-fluorouracil: frequency of the common IVS 14 + 1 G > A mutation causing DPD deficiency. *Clin Cancer Res* **7** : 1149-1153, 2001
14) Villafranca E, Okruzhnov Y, Brugarolas A, et al : Polymorphisms of the repeated sequences in the enhancer region of the thymidylate synthase gene promoter may predict downstaging after preoperative chemoradiation in rectal cancer. *J Clin Oncol* **19** : 1779-1786, 2001
15) Gupta E, Safa AR, Ratain MJ, et al : Pharmacokinetic modulation of irinotecan and metabolites by cyclosporin A. *Cancer Res* **56** : 1309-1314, 1996
16) Horio M, Gottesman MM, Pastan I : ATP-dependent transport of vinblastine in vesicles from human multidrug-resistant cells. *Proc Natl Acad Sci U S A* **85** : 3580-3584, 1988
17) Tanabe M, Ieiri I, Otsubo K, et al : Expression of P-glycoprotein in human placenta: relation to genetic polymorphism of the multidrug resistance (MDR)-1 gene. *J Pharmacol Exp Ther* **297** : 1137-1143, 2001
18) Hoffmeyer S, Burk O, Brinkmann U, et al : Functional polymorphisms of the human multidrug-resistance gene : multiple sequence variations and correlation of one allele with P-glycoprotein expression and activity in vivo. *Proc Natl Acad Sci U S A* **97** : 3473-3478, 2000
19) Sakaeda T, Nakamura T, Okumura K, et al : MDR 1 genotype-related pharmacokinetics of digoxin after single oral administration in healthy Japanese subjects. *Pharm Res* **18** : 1400-1404, 2001
20) Nakamura T, Sakaeda T, Okumura K, et al : Effect of the mutation (C 3435 T) at exon 26 of the MDR 1 gene on expression level of MDR 1 messenger ribonucleic acid in duodenal enterocytes of healthy Japanese subjects. *Clin Pharmacol Ther* **71** : 297-303, 2002
21) Tang K, Ngoi SM, Lee CG, et al : Distinct haplotype profiles and strong linkage disequilibrium at the MDR 1 multidrug transporter gene locus in three ethnic Asian populations. *Pharmacogenetics* **12** : 437-450, 2002
22) Chowbay B, Cumaraswamy S, Lee EJ, et al : Genetic polymorphisms in MDR 1 and CYP 3 A 4 genes in Asians and the influence of MDR 1 haplotypes on cyclosporin disposition in heart transplant recipients. *Pharmacogenetics* **13** : 89-95, 2003

23) Kim RB, Leake BF, Wilkinson GR, et al : Identification of functionally variant MDR 1 alleles among European Americans and African Americans. *Clin Pharmacol Ther* **70** : 189-199, 2001
24) Kurata Y, Ieiri I, Otsubo K, et al : Role of human MDR 1 gene polymorphism in bioavailability and interaction of digoxin, a substrate of P-glycoprotein. *Clin Pharmacol Ther* **72** : 209-219, 2002
25) Siegmund W, Ludwig K, Cascorbi I, et al : The effects of the human MDR 1 genotype on the expression of duodenal P-glycoprotein and disposition of the probe drug talinolol. *Clin Pharmacol Ther* **72** : 572-583, 2002
26) Johne A, Kopke K, Roots I, et al : Modulation of steady-state kinetics of digoxin by haplotypes of the P-glycoprotein MDR 1 gene. *Clin Pharmacol Ther* **72** : 584-594, 2002
27) Morita N, Yasumori T, Nakayama K : Human MDR 1 polymorphism: G 2677 T/A and C 3435 T have no effect on MDR 1 transport activities. *Biochem Pharmacol* **65** : 1843-1852, 2003
28) Chu XY, Kato Y, Sugiyama Y, et al : Biliary excretion mechanism of CPT-11 and its metabolites in humans: involvement of primary active transporters. *Cancer Res* **58** : 5137-5143, 1998
29) Sugiyama Y, Kato Y, Chu X : Multiplicity of biliary excretion mechanisms for the camptothecin derivative irinotecan (CPT-11), its metabolite SN-38, and its glucuronide: role of canalicular multispecific organic anion transporter and P-glycoprotein. *Cancer Chemother Pharmacol* **42** Suppl : S 44-49, 1998
30) Iyer L, Das S, Ratain MJ, et al : UGT 1 A 1•28 polymorphism as a determinant of irinotecan disposition and toxicity. *Pharmacogenomics J* **2** : 43-47, 2002
31) Mathijssen RH, van Alphen RJ, Sparreboom A, et al : Clinical pharmacokinetics and metabolism of irinotecan (CPT-11). *Clin Cancer Res* **7** : 2182-2194, 2001
32) Horikawa M, Kato Y, Sugiyama Y : Reduced gastrointestinal toxicity following inhibition of the biliary excretion of irinotecan and its metabolites by probenecid in rats. *Pharm Res* **19** : 1345-1353, 2002
33) Tirona RG, Leake BF, Kim RB, et al : Polymorphisms in OATP-C: identification of multiple allelic variants associated with altered transport activity among European-and African-Americans. *J Biol Chem* **276** : 35669-35675, 2001
34) Nishizato Y, Ieiri I, Sugiyama Y, et al : Polymorphisms of OATP-C (SLC 21 A 6) and OAT 3 (SLC 22 A 8) genes: consequences for pravastatin pharmacokinetics. *Clin Pharmacol Ther* **73** : 554-565, 2003
35) Evans WE, Relling MV : Pharmacogenomics : translating functional genomics into rational therapeutics. *Science* **286** : 487-491, 1999
36) Innocenti F, Ratain MJ : Update on pharmacogenetics in cancer chemotherapy. *Eur J Cancer* **38** : 639-644, 2002
37) 家入一郎：トランスポーターの臨床的意義．ファルマシア **39** : 427-430, 2003

Functional analysis of single nucleotide polymorphisms of hepatic organic anion transporter OATP1B1 (OATP-C)

Megumi Iwai[a], Hiroshi Suzuki[a], Ichiro Ieiri[b], Kenji Otsubo[b] and Yuichi Sugiyama[a]

Objective **Two kinds of single nucleotide polymorphism (SNP; Asn130Asp and Val174Ala) are frequently observed in the liver specific transporter, organic anion transporting polypeptide 1B1 (OATP1B1/OATP-C) gene. Although these two SNPs occur independently in European-Americans, Val174Ala is mostly associated with Asn130Asp in Japanese. Our previous in-vivo studies in Japanese subjects indicated that the non-renal clearance of pravastatin was decreased to 13% of that in wild-type subjects (Nishizato *et al. Clin Pharmacol Ther* 2003;73(6):554–564). The purpose of the present study is to characterize the function of SNPs variants of OATP1B1 in cDNA transfected cells.**

Methods **The localization and transport activity were analyzed in HEK293 cells stably expressing wild-type OATP1B1 (OATP1B1*1a), OATP1B1*1b (Asn130Asp), OATP1B1*5 (Val174Ala) and OATP1B1*15 (Asn130Asp and Val174Ala). To characterize the intrinsic V_{max}, observed V_{max} in uptake study were normalized by the expression level estimated from Western blotting.**

Results **All SNP variants are predominantly located on the cell surface. No significant alteration was observed in K_m values for the transport of 17β-estradiol 17β-D-glucuronide ($E_2$17βG), a typical substrate of OATP1B1, among these SNP variants. However, the normalized V_{max} value for OATP1B1*15 was drastically decreased to less than 30% compared with OATP1B1*1a. In contrast, the transport activity of OATP1B1*1b (Asn130Asp) and OATP1B1*5 (Val 174Ala) was similar to that of OATP1B1*1a.**

Conclusions **These results are consistent with the results of our previous clinical studies. It is thus suggested that in-vivo disposition may be predicted from in-vitro results using recombinant transporters. *Pharmacogenetics* 14:749–757 © 2004 Lippincott Williams & Wilkins**

Pharmacogenetics 2004, 14:749–757

Keywords: OATP1B1, SNPs, haplotype, hepatic transport, organic anion

[a]Graduate School of Pharmaceutical Sciences, The University of Tokyo, Tokyo and [b]Department of Hospital Pharmacy, Faculty of Medicine, Tottori University, Yonago, Japan.

This work was supported by a grant-in-aid from the Ministry of Education, Science, Culture and Sports for the 21st Century Center of Excellence program and a Health and Labour Sciences Research Grant from Ministry of Health, Labour and Welfare for the Research on Advanced Medical Technology.

Correspondence and requests for reprints to Yuichi Sugiyama, PhD, Professor and Chair, Department of Molecular Pharmacokinetics, School of Pharmaceutical Sciences, The University of Tokyo, 7-3-1 Hongo, Bunkyo-ku, Tokyo 113-0033, Japan.
Tel: +81-3-5841-4770; fax: +81-3-5841-4766;
e-mail: sugiyama@mol.f.u-tokyo.ac.jp

Received May 8, 2004
Accepted June 15, 2004

Introduction

The administration of the same amount of certain drugs to individuals often results in variability in drug disposition. This is partly due to the presence of hereditary differences, such as single nucleotide polymorphisms (SNPs), in the genes encoding drug metabolizing enzymes and/or transporters [1,2]. Although the correlation between genotype and phenotype has been studied extensively as far as drug metabolizing enzymes are concerned [3,4], only limited information is available on the SNPs of the genes of drug transporters which are responsible for drug disposition [5].

Some pieces of information are available on organic anion transporting polypeptide 1B1 (OATP1B1/OATP-C), a basolaterally located transporter, which is responsible for the hepatic uptake of a series of organic anions, including 17β-estradiol 17β-D-glucuronide ($E_2$17βG), estrone-3-sulfate (E_1S), taurocholate, conjugated bilirubin, and anionic drugs such as pravastatin, from the portal vein to hepatocytes [6–11].

At present, several kinds of SNP variants have been identified in the human OATP1B1 gene. As far as the nomenclature of OATP1B1 variants is concerned, the cDNA sequence reported by Konig *et al.* [7] is designated as OATP1B1*1a. Recently, using stably transfected MDCKII cells, Michalski *et al.* [12] have identified a naturally occurring mutation in the OATP1B1 gene leading to an impairment of the protein mutation with reduced localization and abolished transport activity. The missorting to the membrane surface was also confirmed by intracellular localization of the mutant protein in the cryosections of human liver [12]. Tirona *et al.* [13] have identified the SNPs in the OATP1B1 gene in European-American

and African-American subjects, and examined their function by transfecting the cDNAs into HeLa cells. Although they found that the expression levels of OATP1B1*3 (Val62Ala), OATP1B1*5 (Val174Ala), OATP1B1*6 (Ile353Thr) and OATP1B1*9 (Gly488Ala) were similar to that of OATP1B1*1a by Western blot analysis of cell lysate, their degree of expression on the cell surface was reduced and consequently, a reduction in the transport of $E_2$17βG and E_1S has been observed [13]. In contrast, using HEK293 cells transiently expressing OATP1B1, Nozawa *et al.* [14] reported that the cellular localization and transport function of OATP1B1*5 were no different from that of OATP1B1*1a, when E_1S is used as a ligand. The cells used to determine the function of OATP1B1 were different in the two reports, and it remains to be clarified whether the function of OATP1B1*5 is similar to that of OATP1B1*1a [14].

Recently, Nozawa *et al.* [14] found a novel OATP1B1 allele, OATP1B1*15, possessing both Asn130Asp and Val174Ala variants in Japanese subjects. OATP1B1*15 is different from OATP1B1*1b which is associated with Asn130Asp, but not with Val174Ala, and OATP1B1*5 which is associated with Val174Ala, but not with Asn130Asp. Although the allelic frequency of OATP1B1*5 is 14% in European-Americans, no Japanese subjects with this allele were found in our previous study [15]. In contrast, most of the Japanese subjects who have Val174Ala also have Asn130Asp and, therefore, a clear ethnic difference was observed in the frequency of the haplotype. However, no information is available on the in-vitro function of OATP1B1*15. To investigate the effect of SNPs on drug disposition, we recently reported the disposition of pravastatin, an HMG-CoA reductase inhibitor which is taken up by OATP1B1, in healthy Japanese subjects [15]. We found that the non-renal clearance of pravastatin in healthy Japanese subjects with the OATP1B1*15 allele is reduced to 13% of the wild-type (OATP1B1*1a). However, in-vitro evidence to support this in-vivo result is still lacking. In the present study, we constructed HEK293 cells stably expressing OATP1B1*1a, OATP1B1*1b, OATP1B1*5 and OATP1B1*15 and characterized their cellular localization and transport activity.

Material and methods

Materials

[^{3}H] $E_2$17βG (45.0 μCi/nmol) and [^{3}H] E_1S (46.0 μCi/nmol) were purchased from New England Nuclear (Boston, MA, USA). All other chemicals were commercially available and of reagent grade.

Construction of OATP1B1 SNP variants expressed in HEK293 cells

Human OATP1B1*1b (Asn130Asp) cDNA was subcloned into pcDNA3.1 (+) (Zeocin) (Invitrogen, Carlsbad, CA, USA). To construct the other SNP variants, point mutations were introduced by using the QuickChange site-directed mutagenesis kit (Stratagene, La Jolla, CA, USA). The introduction of the mutations was verified by full sequencing. Wild-type and SNP variants of OATP1B1 in pcDNA3.1 were transfected to HEK293 cells grown on a 12-well plate with Fugene 6 (Roche Diagnostics Corporation, Indianapolis, IN, USA) according to the manufacturer's instructions. Then, HEK293 cells were selected by 200 μg/ml Zeocin and colonies were picked up and the colonies which had the highest transport activities were used in the functional analysis. HEK293 cells stably expressing OATP1B1 were cultured in low-glucose Dulbecco's modified Eagle's medium (GIBCO BRL, Gaithersburg, MD, USA) after addition of 10% fetal bovine serum, penicillin (100 U/ml) and streptomycin (100 μg/ml), zeocin (200 μg/ml) (Invitrogen) at 37°C with 5% CO_2, and 95% humidity. Sodium butyrate (5 mM) was added to the medium 24 hr before all experiments to induce the expression of OATP1B1.

Immunocytochemical staining

HEK293 cells stably expressing OATP1B1 were grown on a poly-L-lysine coated cover glass (Micro cover glass, 18 × 18 mm and 0.12–0.17 mm thick, Matsunami Glass Ind., Osaka, Japan). After fixation in −20°C methanol for 10 min and permeabilization in 1% Triton-X in phosphate-buffered saline (PBS) for 10 min, cells were incubated with the polyclonal antibody against OATP1B1 [16] diluted 50-fold in PBS for 1 h, washed three times with PBS, and then incubated with goat anti-rabbit immunoglobulin G (IgG; Alexa 488, Molecular Probes, Inc., Eugene, OR, USA) diluted 250-fold in PBS for 1 h. The localization of OATP1B1 protein was visualized by confocal lazer microscopy (Zeiss LSM-510; Carl Zeiss Inc., Thornwood, NY, USA).

Cell surface biotinylation

HEK293 cells stably expressing OATP1B1s were grown on 24-well plates. Cells were washed with ice-cold PBS containing 0.1 mM $CaCl_2$ and 1 mM $MgCl_2$ (PBS-Ca/Mg), then incubated twice with NHS-SS-biotin (1.5 mg/ml; Pierce Biotechnology, Inc., Rockford, IL, USA) at 4°C for 20 min. Then, the cells were washed with PBS Ca^{2+}/Mg^{2+} containing glycine (100 mM) and incubated with the same buffer for 20 min at 4°C. After removing the buffer, cells were disrupted with 50 μl lysis buffer (50 mM Tris, 150 mM NaCl, 5 mM ethylenediaminetetraacetic acid (EDTA), 1% Triton-X-100, pH 7.5) containing 1% sodium dodecyl sulfate (SDS) and protease inhibitor (0.1 mM phenylmethylsulfonyl fluoride) at 4°C for 30 min. To reduce the SDS concentration, samples were diluted with 450 μl of lysis buffer. Then, 50 μl of streptavidin-agarose beads (Pierce) was added to the lysate, and incubated at 4°C overnight with end-over-end rotation. Following centri-

fugation, the beads were washed three times with lysis buffer, twice with high salt lysis buffer (50 mM Tris, 500 mM NaCl, 5 mM EDTA, 0.1% Triton-X-100, pH 7.5), and once with low salt lysis buffer (50 mM Tris, pH 7.5). The biotinylated proteins were released by incubation with 40 µl 3× SDS loading buffer (BioLabs, Hitchin, UK) diluted to 1× SDS with PBS for 5 min at 60°C. Samples for total cell lysates (15 µl) and biotinylated proteins (2 µl) were subjected to the Western blot analysis.

Western blotting

Membrane fractions were prepared from HEK293 cells stably expressing OATP1B1 as described previously [17]. These crude membrane fractions were diluted with 3× SDS loading buffer and separated on 7% SDS-polyacrylamide gel with a 4.4% stacking gel. Proteins were transferred electrophoretically to a nitrocellulose membrane (Millipore, Bedford, MA, USA) using a blotter (Bio-Rad Laboratories, Richmond, CA, USA) at 15 V for 1 h. The membrane was blocked with 2.5% skimmed milk for 1 h at room temperature. Then, the membrane was incubated for 1 hr at room temperature with 500-fold diluted anti-OATP1B1 rabbit serum. For the detection of OATP1B1, the membrane was allowed to bind to 5000-fold diluted horseradish peroxidase-labeled anti-rabbit IgG antibody (Amersham Pharmacia Biotech, Amersham, UK) for 1 h at room temperature. The enzyme activity was assessed using ECL Plus Western blotting Starter Kit (Amersham Biosciences, Inc.) with luminescent image analyzer (LAS-1000 plus, Fuji Film). The molecular weight was determined using a prestained protein marker (New England BioLabs, Beverly, MA).

Transport studies

Transport studies of [^{3}H] $E_2$17βG and [^{3}H] E_1S were carried out as described previously [18]. Uptake was initiated after cells were washed twice and preincubated with Krebs–Henseleit buffer at 37°C for 15 min. The Krebs–Henseleit buffer consists of 118 mM NaCl, 23.8 mM $NaHCO_3$, 4.83 mM KCl, 0.96 mM KH_2PO_4, 1.20 mM $MgSO_4$, 12.5 mM HEPES, 5 mM glucose, and 1.53 mM $CaCl_2$, adjusted to pH 7.4. After the removal of the incubation buffer, the uptake was terminated at designed times by adding ice-cold Krebs–Henseleit buffer, dissolved in 500 µl 0.2 N NaOH, and kept overnight. Aliquots (450 µl) were transferred to scintillation vials after adding 100 µl 1 N HCl. The radioactivity associated with the cells and medium was determined in a liquid scintillation counter after addition of 2 ml scintillation fluid (NACALAI TESQUE, Kyoto, Japan). The remaining 50 µl of the aliquots of the cell lysate was used to determine the protein concentration by the method of Lowry with bovine serum albumin as a standard.

Ligand uptake is given as the volume of distribution (µl/mg of protein) determined as the amount of ligand associated with the cells (pmol/mg of protein) divided by the medium concentration (pmol/µl). Specific uptake was obtained by subtracting the uptake into vector-transfected cells from the uptake into cDNA-transfected cells. Kinetic parameters were obtained using the following equation.

$$v = \frac{V_{max} \times S}{K_m + S} + P_{dif} \times S$$

where v is the uptake velocity of the substrate (pmol/min/mg of protein), S is the substrate concentration in the medium (µM), K_m is the Michaelis–Menten constant (µM), V_{max} is the maximum uptake rate (pmol/min/mg of protein) and P_{dif} is the nonspecific uptake clearance (µl/min/mg of protein). Fitting was performed by the nonlinear least-squares method using MULTI program [19] with the Damping Gauss Newton Method algorithm.

Results

Cellular localization of human OATP1B1

The localization of OATP1B1 SNP variants was investigated by immunocytochemical staining (Fig. 1). It has been previously reported that the localization of OATP1B1*1a and OATP1B1*1b is limited to the cell surface in transiently transfected HEK293 cells [14]. It was found that OATP1B1*1a and OATP1B1*1b are localized on the cell surface in HEK293 cells (Fig. 1), which is consistent with the previous report [14]. Moreover, cellular surface localization was identified for OATP1B1*5 and OATP1B1*15. No OATP1B1 derived staining was observed in vector-transfected HEK293 cells (Fig. 1).

The cellular localization of SNP variants was also confirmed by the cell surface biotinylation method (Fig. 2). The ratio of the biotinylated OATP1B1 in the cell surface fraction to that in the whole cell lysate was analyzed by densitometric analysis. This ratio of OATP1B1*1b, OATP1B1*5 and OATP1B1*15 was almost the same as that of OATP1B1*1a, and they were 64, 98 and 103% of OATP1B1*1a, respectively (Fig. 2). The efficiency of fractionation of cell surface protein was confirmed by an immunodetectable intracellular protein (calnexin).

Western blotting

Western blotting was performed using crude membrane from HEK293 transfectants, and the protein expression level of each OATP1B1 SNP variant was estimated by quantifying the OATP1B1 band densities (Fig. 3). Although the expression level of each SNP variant differed, the molecular mass was approximately 80 kDa (Fig. 3). OATP1B1*1b and OATP1B1*5 showed a

Fig. 1

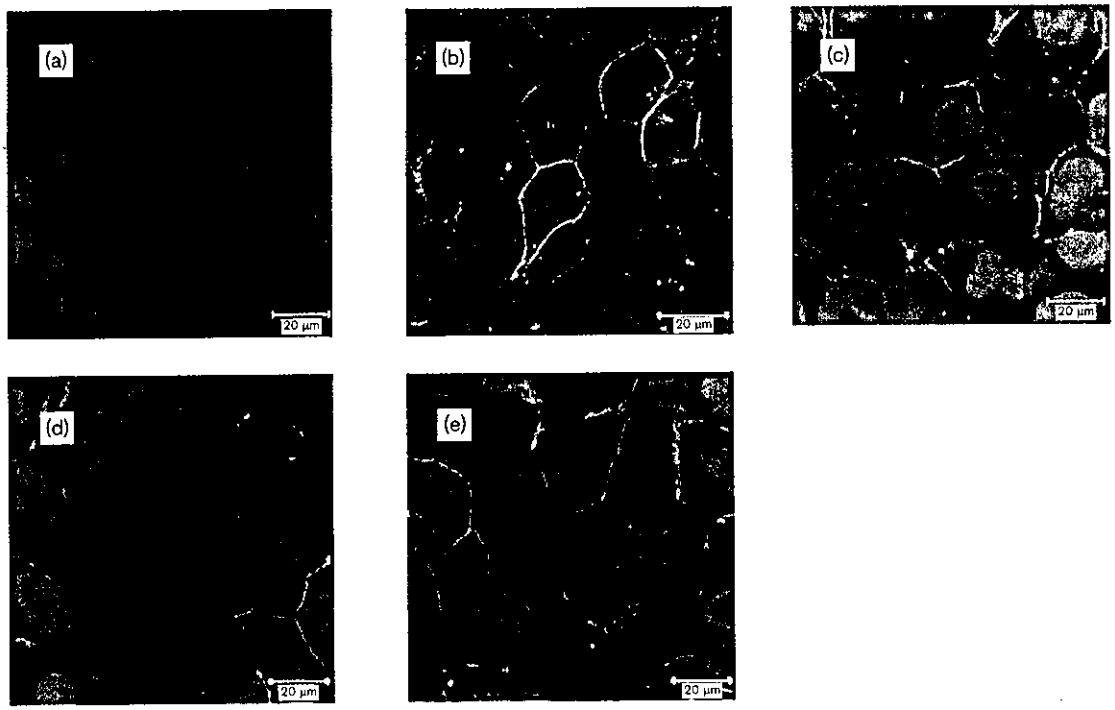

Immunolocalization of OATP1B1 allelic variants in HEK293 cells. OATP1B1 (green fluorescence) and nuclei (red fluorescence) were stained using the polyclonal antibody for OATP1B1 and propidium iodide, respectively. (a–e) represent the staining of vector-transfected, OATP1B1*1a-, OATP1B1*1b-, OATP1B1*5- and OATP1B1*15-expressing HEK293 cells, respectively. Bars = 20 μm.

Fig. 2

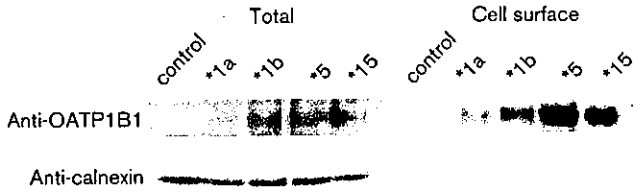

Cell surface biotinylation of OATP1B1 allelic variants. Total cell lysate protein containing both cell surface and intracellular protein (15 μl of solution) (left panel) and biotinylated protein (2 μl of solution) (right panel) was subjected to SDS–polyacylamide gel electrophoresis (PAGE) (7%). The membrane was incubated with anti-OATP1B1 polyclonal antibody (top panel). After washing, the membrane was incubated with anti-calnexin antibody (bottom panels). The band density against OATP1B1 was quantified in a luminescent image analyzer.

similar expression level to that of OATP1B1*1a (130% and 140%, respectively). In contrast, the expression level of OATP1B1*15 was approximately 11-fold higher than that of OATP1B1*1a. These values were used to normalize the transport activities of each OATP1B1 variant.

Uptake experiments

The time-profiles for the uptake of [^{3}H] $E_2$17βG and [^{3}H] E_1S by HEK293 cells stably expressing OATP1B1s are shown in Fig. 4. Significantly greater uptake of these compounds was observed in the cDNA-transfected cells compared with vector-transfectant (Fig. 4). Moreover, kinetic parameters were analyzed using [^{3}H] $E_2$17βG as a substrate (Fig. 5). The data for the saturation studies (Fig. 5) are given after correcting the uptake into vector-transfected cells. However, even after subtracting the transport into the vector-transfected cells, it was necessary for us to assume the presence of P_{dif} for the analysis, presumably due to the experimental deviations in the uptake between the vector-transfected and OATP1B1 cDNA-transfected cells. The K_m values of OATP1B1*1a, OATP1B1*1b, OATP1B1*5, and OATP1B1*15 were comparable, and they were 4.26 ± 1.66, 3.96 ± 1.29, 5.90 ± 2.00 and 4.07 ± 2.48 μM, respectively (Fig. 5). The apparent V_{max} values of these variants were 35.7 ± 12.9, 49.3 ± 14.9, 46.6 ± 15.1 and 28.8 ± 16.1 pmol/min/mg cellular protein, respectively. In order to determine the V_{max} values for each OATP1B1 molecule, it is essential to consider the cell surface expression level of OATP1B1s. Table 1 shows these values obtained by dividing the V_{max} values per mg cellular

Fig. 3

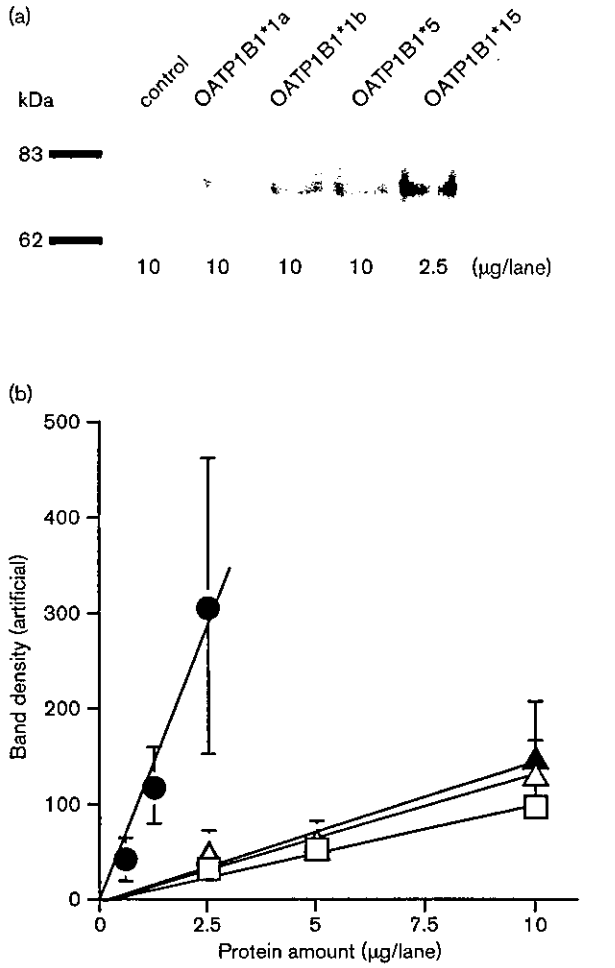

Quantification of the expression level of OATP1B1 in HEK293 cells. Crude membrane obtained from HEK293 cells was separated by SDS–PAGE (7%). The applied amount of protein was 10 μg, 10 μg, 10 μg, 10 μg and 2.5 μg for OATP1B1*1a, OATP1B1*1b, OATP1B1*5 and OATP1B1*15, respectively. OATP1B1 proteins were detected using horseradish peroxidase-labeled anti-rabbit IgG after incubation with the polyclonal antibody for OATP1B1 (a). Quantification of the OATP1B1 expression level was performed in a luminescent image analyzer. In (b), each point and bar represents the mean ± SE of three independent experiments, □, OATP1B1*1a expressing cells; △, OATP1B1*1b expressing cells; ▲, OATP1B1*5 expressing cells; ●, OATP1B1*15 expressing cells.

protein by the OATP1B1 expression level estimated by Western blotting (Fig. 3). For OATP1B1*15, the intrinsic V_{max} value was reduced to 7.3% of OATP1B1*1a, whereas the V_{max} values for OATP1B1*5 and OATP1B1*1b were similar to OATP1B1*1a.

Transport properties of other OATP1B1*15 clones

In order to confirm the results that the transport function of OATP1B1*15 is reduced compared to the wild-type transporter, further analysis was performed by using two other OATP1B1*15 clones. The results of the Western blot analysis and uptake study using OATP1B1*1a and other OATP1B1*15 clones (OATP1B1*15′ and OATP1B1*15″) are shown in Fig. 6. The expression level of OATP1B1*15′ and OATP1B1*15″ clones were 75 and 180% that of OATP1B1 *1a. OATP1B1*15′- and OATP1B1*15″-mediated transport was reduced to 21 and 30% of OATP1B1*1a, respectively, after correction of their protein expression levels (Fig. 6).

Discussion

In the present report, we focused on the function of Asn130Asp and Val174Ala SNP variants of human OATP1B1. The localization and transport activity were analyzed for OATP1B1*1a, OATP1B1*1b (Asn130Asp), OATP1B1*5 (Val174Ala) and OATP1B1*15 (Asn-130Asp and Val174Ala) using stably transfected HEK293 cells. The presence of Asn130Asp and Val-174Ala variations in the OATP1B1 gene has been reported in several ethnic groups. Among the SNP variations, Asn130Asp is observed at the highest frequency in European-Americans, African-Americans and Japanese and allelic frequencies of 30%, 74% and 60~63%, respectively [13–15]. Although Val174Ala commonly appeared in European-Americans and Japanese with an allele frequency of 14% and 11~16%, respectively, the frequency in African-Americans is relatively low (2%) [13]. Interestingly, the allelic frequency of OATP1B1*5, which has only the Val174Ala variation, is relatively low in Japanese (0~0.7%), which is in contrast to the high frequency of OATP1B1*5 in European-Americans (14.0%) [13–15]. The Japanese subjects with Val174Ala also have Asn130Asp, and therefore, the presence of an interethnic difference in haplotype formation has been demonstrated between European-Americans and Japanese [13–15].

We recently reported that the non-renal clearance of pravastatin, an OATP1B1 substrate, in the Japanese subjects with the OATP1B1*15/*1b allele was reduced to 55% that in OATP1B1*1b/*1b subjects [15]. In addition, the same value in an OATP1B1*15/*15 subject was reduced to 14% of the control subjects [15]. It is possible that the reduction in OATP1B1 function by SNP variations is responsible for this functional alteration. The reduction in the function of membrane transporters may be accounted for by considering several factors: such as (1) the reduction in the intrinsic activity per transporter molecule, due to the reduced affinity for substrates and/or the reduction in the translocation ability; (2) altered protein expression due to the altered stability of mRNA and/or protein; and (3) impairment of the membrane sorting.

In the present study, we have characterized the SNP variants of OATP1B1 from the standpoints described above. The localization of SNP variants was analyzed

Fig. 4

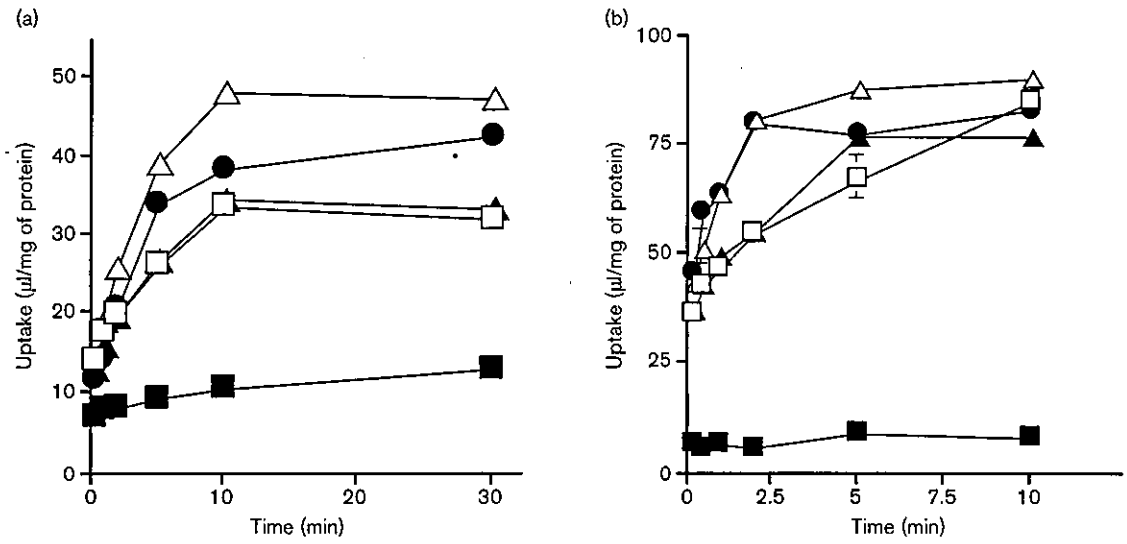

Time-profiles for the transport of [^{3}H] $E_2$17βG and [^{3}H] E_1S by OATP1B1 SNP variants. Time-profiles for the uptake of [^{3}H] $E_2$17βG (100 nM; a), and [^{3}H] E_1S (50 nM; b) were examined. Each point and vertical bar represents the mean ± SE of three independent determinations. Key: ■; vector-transfected cells, □; OATP1B1*1a expressing cells, △; OATP1B1*1b expressing cells, ▲; OATP1B1*5 expressing cells, ●; OATP1B1*15 expressing cells.

by immunocytochemical staining and cell surface biotinylation methods. As shown in Fig. 1, most of the SNP variant molecules were located on the plasma membrane. In addition, these results were confirmed by the biotinylation assay (Fig. 2). The fact that OATP1B1*1a, OATP1B1*1b and OATP1B1*5 are mostly located on the plasma membrane is consistent with the previous results reported in transiently transfected HEK293 cells. However, the band density of OATP1B1*15 was not much higher than that of OATP1B1*1a/1b in Fig. 2. At the present moment, we do not have any good reason for this discrepancy between Figs 2 and 3. In obtaining the results shown in Fig. 2, the applied amount was not normalized with respect to the amount of lysate protein due to the difficulties in measuring the protein concentrations in the lysate solution containing SDS as a detergent. It is still possible that the applied amount differs between clones, although experiments were performed under the same conditions for all OATP1B1 variants. Since the degree of expression of OATP1B1 proteins is quite important in the interpretation of the experimental results, we also examined the transport mediated by OATP1B1*15 by using two other clones (Fig. 6) as discussed later in detail.

To compare the intrinsic transport activity of SNP variants of OATP1B1, the uptake of typical substrates was examined. The K_m values for $E_2$17βG were similar, indicating that the SNPs do not affect the affinity for $E_2$17βG (Fig. 5). The V_{max} values for $E_2$17βG were normalized by the protein expression level estimated by Western blotting. Although the V_{max} values defined for the amount of cellular protein were almost identical for OATP1B1*1a, OATP1B1*1b, OATP1B1*5 and OATP1B1*15, the intrinsic V_{max} for OATP1B1*15, defined for the expressed OATP1B1 protein level, was reduced to 7.3% of OATP1B1*1a (Table 1). Since the non-renal clearance of pravastatin, which is largely accounted for by biliary excretion clearance, in Japanese subjects with the OATP1B1*15 allele was reduced to 13% of that in OATP1B1*1a subjects [15], the degree of reduction in the transport activity is similar to the present in-vitro results. In contrast to the reduction in the transport activity of OATP1B1*15, no significant difference was observed in the kinetic parameters between OATP1B1*1a, OATP1B1*1b and OATP1B1*5 (Fig. 5).

The results that the transport function of OATP1B1*1a and *1b is similar for $E_2$17βG is consistent with the previous report by Michalski *et al.* [12]. In contrast, they found that the transport function of OATP1B1*1b is higher and lower for bromosulfophthalein and taurocholic acid, respectively, compared to OATP1B1*1a [12]. Since it is possible that the effect of SNPs on the transport activity is substrate-specific, it is important for us to examine the transport of pravastatin by OATP1B1 variants. Although we examined the uptake of pravastatin, we could not detect any significant OATP1B1-

Fig. 5

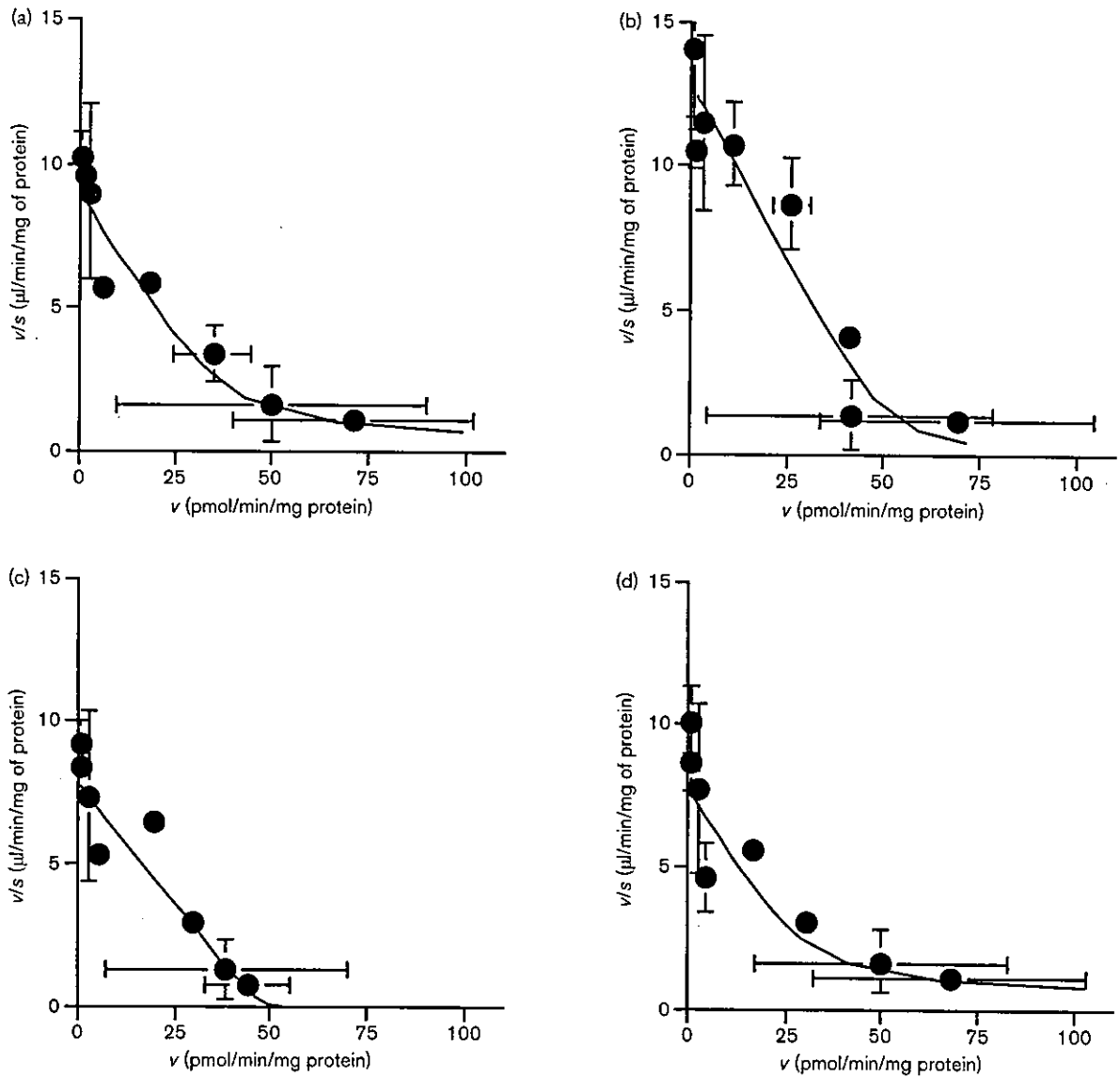

Eadie–Hofstee plot for OATP1B1-mediated uptake of [^{3}H] $E_2$17βG. The transport velocity determined by examining the uptake of [^{3}H] $E_2$17βG for 2 min was determined in OATP1B1*1a (a), OATP1B1*1b (b), OATP1B1*5 (c), and OATP1B1*15 (d) expressing HEK293 cells. Each point and bar represents the mean ± SE of three independent experiments. The solid line represents the fitted line. The OATP1B1 mediated transports were obtained by subtracting the transport velocity in vector-transfected cells from those in OATP1B1 SNP variants-expressed cells.

Table 1 Kinetic parameters for the transport of [^{3}H] $E_2$17βG

Genotype	K_m (μM)	V_{max} (pmol/min/mg protein)	P_{df} (μl/min/mg protein)	V_{max}/K_m (μl/min/mg protein)	Expression amount (% of *1a)	Corrected V_{max} (% of *1a)
OATP1B1*1a	4.3 ± 1.7	35.7 ± 12.9	0.644 ± 0.306	8.38 ± 4.46	100	100
OATP1B1*1b	4 ± 1.3	49.3 ± 14.9	0.222 ± 0.344	12.4 ± 5.5	130	110
OATP1B1*5	5.9 ± 2.0	46.6 ± 15.1	0.015 ± 0.2762	7.9 ± 3.7	140	93
OATP1B1*15	4.07 ± 2.5	28.8 ± 16.1	0.738 ± 0.399	7.06 ± 5.84	1100	7.3

Data shown in Fig. 5 were analyzed to determine the kinetic parameters. Moreover, the V_{max} values were normalized by the expression level of OATP1B1 protein determined by the Western blot analysis shown in Fig. 3.

Fig. 6

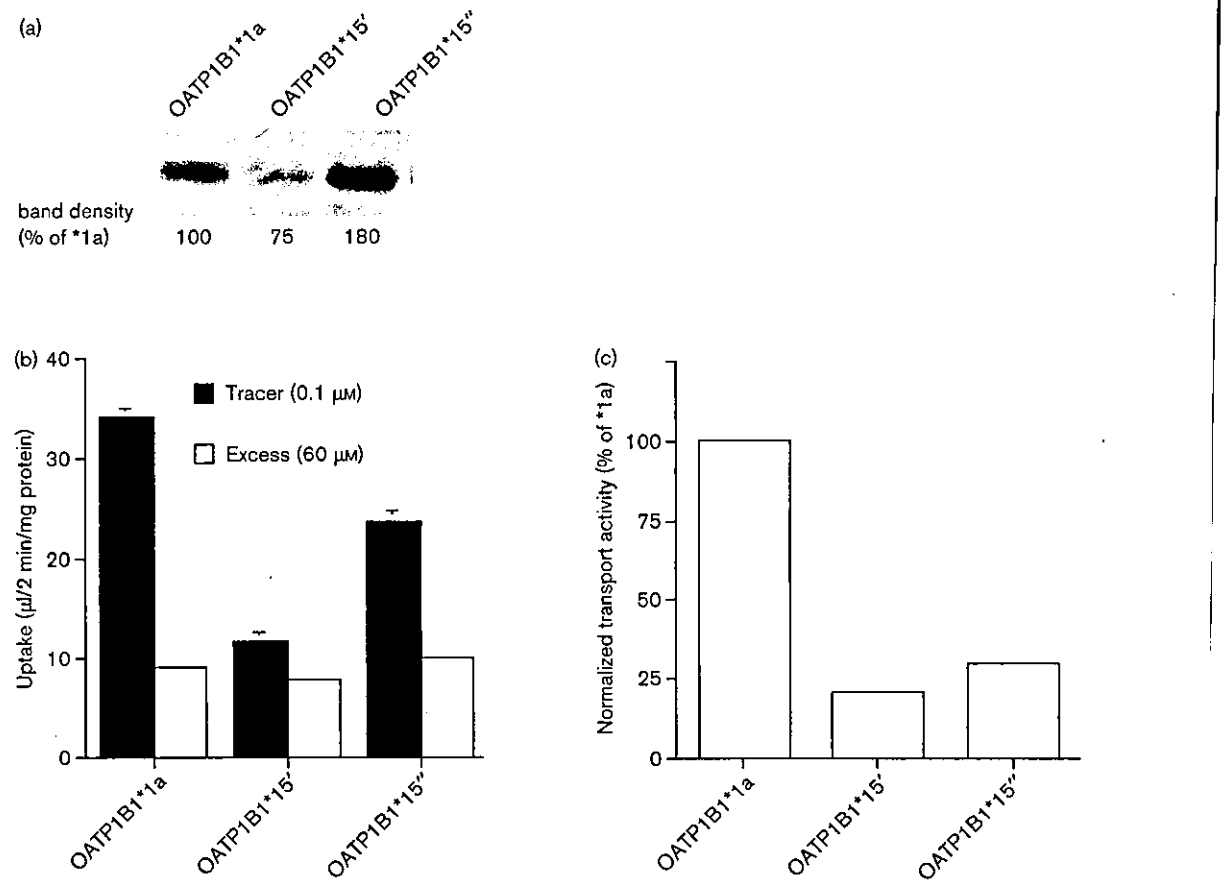

Western blot analysis and uptake study using other OATP1B1*15 clones. The uptake of $E_2$17βG was examined using other two OATP1B1*15 clones. The expression level of OATP1B1 was also determined by the Western blot analysis. (a) Crude membrane (10 μg) obtained from HEK293 cells was separated by SDS–PAGE (7%). OATP1B1 proteins were detected using horseradish peroxidase-labeled anti-rabbit IgG after incubation with the polyclonal antibody for OATP1B1. (b) HEK293 cells expressing OATP1B1*1a, OATP1B1*15 clones 1 and 2 were incubated for 2 min in the presence of [^{3}H] $E_2$17βG with tracer (0.1 μM; closed bar) or excess (60 μM; open bar) concentration of unlabeled $E_2$17βG. Each point and bar represents the mean ± SE of three independent experiments. (c) The transport activity was obtained by subtracting the transport velocity in the presence of excess amount of unlabeled $E_2$17βG from the transport velocity in its absence shown in (b). Then, the normalized transport activity was calculated by normalizing the transport activity by the OATP1B1 expression level estimated from (a).

mediated uptake of this drug due to the low transport activity compared with the background level. This result is consistent with our previous transcellular transport studies with MDCK II monolayer expressing the uptake (OATP1B1) and efflux (MRP2) transporters on the basolateral and apical membrane, respectively; the extent of the basal-to-apical transport of pravastatin was less than 20% of that of $E_2$17βG [16]. It is unfortunate that the transport of pravastatin was not detectable under the present experimental conditions. However, our previous in-vivo findings that the non-renal clearance of pravastatin is much lower in OATP1B1*15 subjects [15] is consistent with the reduced transport function of OATP1B1*15 determined in the present study.

Focusing on the OATP1B1*5 allele, two groups have reported contradictory results. Nozawa *et al.* [14] demonstrated that the localization and transport activity of OATP1B1*5 was similar to that of OATP1B1*1a using HEK293 as host cells, which is consistent with the present results (Fig. 1). In contrast, Tirona *et al.* [13] used HeLa cells and observed a reduction in the cell surface expression of OATP1B1*5. This discrepancy may be due to a difference in the membrane targeting mechanism between HEK293 and HeLa cells. Although we also found the membrane localization of OATP1B1*15 in our HEK 293 cells, we need to be careful in expecting in-vivo cellular localization from the results of in-vitro expression system. Indeed, the difference in the cellular localization of transporters was reported previously [20–23]. It is also difficult for us to determine the in-vivo function of OATP1B1*5 from

the drug disposition due to the low frequency of OATP1B1*5 in Japanese subjects.

Finally, the expression level of SNP variants of OATP1B1 needs to be discussed. The expression level of the OATP1B1*15 clone analyzed in the present study was 11 times higher than that of OATP1B1*1a. In order to demonstrate that this high expression is not a unique characteristic of OATP1B1*15 and to confirm that the transport function of OATP1B1*15 is indeed reduced compared with the wild-type OATP1B1, we determined the expression level and transport properties of OATP1B1*15 in other clones, which were picked up during the selection in the presence of zeocin. The OATP1B1*15 expression level in two other clones was 75 and 180% that of OATP1B1*1a, indicating that high expression is not necessarily associated with the OATP1B1*15 variation (Fig. 6). In addition, their intrinsic transport activity for $E_2$17βG was also reduced to 21 and 30% of OATP1B1*1a (Fig. 6), after correction of their protein expression levels. Using these two clones, it was confirmed that the transport function is indeed reduced in OATP1B1*15.

In conclusion, we analyzed the function of four OATP1B1 SNPs variants. Although all the SNP variants examined in the present study were located on the cellular membrane, the intrinsic V_{max} value for $E_2$17βG in the OATP1B1*15 variant was reduced to 7.3% that in OATP1B1*1a. The degree of the reduction in V_{max} is similar to that for the non-renal clearance of pravastatin in healthy Japanese subjects with the OATP1B1*15 allele [15]. These results suggest that in-vitro transport experiments with cDNA-transfected HEK293 cells are useful tools for predicting the effects of OATP1B1 SNPs on in-vivo drug disposition.

References

1 Evans WE and Relling MV. Pharmacogenomics: translating functional genomics into rational therapeutics. *Science* 1999; **286**:487–491.
2 Evans WE and McLeod HL. Pharmacogenomics – drug disposition, drug targets, and side effects. *N Engl J Med* 2003; **348**:538–549.
3 Meyer UA and Zanger UM. Molecular mechanisms of genetic polymorphisms of drug metabolism. *Annu Rev Pharmacol Toxicol* 1997; **37**: 269–296.
4 Rodrigues AD and Rushmore TH. Cytochrome P450 pharmacogenetics in drug development: in vitro studies and clinical consequences. *Curr Drug Metab* 2002; **3**:289–309.
5 Hoffmeyer S, Burk O, von Richter O, Arnold HP, Brockmoller J, Johne A, *et al.* Functional polymorphisms of the human multidrug-resistance gene: multiple sequence variations and correlation of one allele with P-glycoprotein expression and activity in vivo. *Proc Natl Acad Sci U S A* 2000; **97**:3473–3478.
6 Hsiang B, Zhu Y, Wang Z, Wu Y, Sasseville V, Yang WP, *et al.* A novel human hepatic organic anion transporting polypeptide (OATP2). Identification of a liver-specific human organic anion transporting polypeptide and identification of rat and human hydroxymethylglutaryl-CoA reductase inhibitor transporters. *J Biol Chem* 1999; **274**:37161–37168.
7 Konig J, Cui Y, Nies AT, Keppler D. A novel human organic anion transporting polypeptide localized to the basolateral hepatocyte membrane. *Am J Physiol Gastrointest Liver Physiol* 2000; **278**:G156–G164.
8 Tamai I, Nezu J, Uchino H, Sai Y, Oku A, Shimane M, *et al.* Molecular identification and characterization of novel members of the human organic anion transporter (OATP) family. *Biochem Biophys Res Commun* 2000; **273**:251–260.
9 Abe T, Kakyo M, Tokui T, Nakagomi R, Nishio T, Nakai D, *et al.* Identification of a novel gene family encoding human liver-specific organic anion transporter LST-1. *J Biol Chem* 1999; **274**:17159–17163.
10 Cui Y, Konig J, Leier I, Buchholz U, Keppler D. Hepatic uptake of bilirubin and its conjugates by the human organic anion transporter SLC21A6. *J Biol Chem* 2001; **276**:9626–9630.
11 Tamai I, Nozawa T, Koshida M, Nezu J, Sai Y, Tsuji A. Functional characterization of human organic anion transporting polypeptide B (OATP-B) in comparison with liver-specific OATP-C. *Pharm Res* 2001; **18**:1262–1269.
12 Michalski C, Cui Y, Nies AT, Nuessler AK, Neuhaus P, Zanger UM, *et al.* A naturally occurring mutation in the SLC21A6 gene causing impaired membrane localization of the hepatocyte uptake transporter. *J Biol Chem* 2002; **277**:43058–43063.
13 Tirona RG, Leake BF, Merino G, Kim RB. Polymorphisms in OATP-C: identification of multiple allelic variants associated with altered transport activity among European- and African-Americans. *J Biol Chem* 2001; **276**:35669–35675.
14 Nozawa T, Nakajima M, Tamai I, Noda K, Nezu J, Sai Y, *et al.* Genetic polymorphisms of human organic anion transporters OATP-C (SLC21A6) and OATP-B (SLC21A9): allele frequencies in the Japanese population and functional analysis. *J Pharmacol Exp Ther* 2002; **302**:804–813.
15 Nishizato Y, Ieiri I, Suzuki H, Kimura M, Kawabata K, Hirota T, *et al.* Polymorphisms of OATP-C (SLC21A6) and OAT3 (SLC22A8) genes: consequences for pravastatin pharmacokinetics. *Clin Pharmacol Ther* 2003; **73**:554–565.
16 Sasaki M, Suzuki H, Ito K, Abe T, Sugiyama Y. Transcellular transport of organic anions across a double-transfected Madin–Darby canine kidney II cell monolayer expressing both human organic anion-transporting polypeptide (OATP2/SLC21A6) and Multidrug resistance-associated protein 2 (MRP2/ABCC2). *J Biol Chem* 2002; **277**:6497–6503.
17 Ogawa K, Suzuki H, Hirohashi T, Ishikawa T, Meier PJ, Hirose K, *et al.* Characterization of inducible nature of MRP3 in rat liver. *Am J Physiol Gastrointest Liver Physiol* 2000; **278**:G438–G446.
18 Sugiyama D, Kusuhara H, Shitara Y, Abe T, Meier PJ, Sekine T *et al.* Characterization of the efflux transport of 17β-D-17β-glucuronide from the brain across the blood-brain barrier. *J Pharmacol Exp Ther* 2001; **298**:316–322.
19 Yamaoka K, Tanigawara Y, Nakagawa T, Uno T. A pharmacokinetic analysis program (multi) for microcomputer. *J Pharmacobiodyn* 1981; **4**:879–885.
20 Masuda S, Saito H, Inui KI. Interactions of nonsteroidal anti-inflammatory drugs with rat renal organic anion transporter, OAT-K1. *J Pharmacol Exp Ther* 1997; **283**:1039–1042.
21 Masuda S, Ibaramoto K, Takeuchi A, Saito H, Hashimoto Y, Inui KI. Cloning and functional characterization of a new multispecific organic anion transporter, OAT-K2, in rat kidney. *Mol Pharmacol* 1999; **55**: 743–752.
22 Gu HH, Ahn J, Caplan MJ, Blakely RD, Levey AI, Rudnick G. Cell-specific sorting of biogenic amine transporters expressed in epithelial cells. *J Biol Chem* 1996; **271**:18100–18106.
23 Folsch H, Ohno H, Bonifacino JS, Mellman I. A novel clathrin adaptor complex mediates basolateral targeting in polarized epithelial cells. *Cell* 1999; **99**:189–198.

Functional Analysis of SNPs Variants of BCRP/ABCG2

Chihiro Kondo,[1] Hiroshi Suzuki,[2] Masaya Itoda,[3] Shogo Ozawa,[3] Jun-ichi Sawada,[3] Daisuke Kobayashi,[4] Ichiro Ieiri,[5] Kazunori Mine,[4] Kenji Ohtsubo,[5] and Yuichi Sugiyama[1,6]

Received February 27, 2004; accepted June 21, 2004

Purpose. The aim of the current study was to identify the effect of single nucleotide polymorphisms (SNPs) in breast cancer resistance protein (BCRP/ABCG2) on its localization, expression level, and transport activity.

Methods. The cellular localization was identified using the wild type and seven different SNP variants of BCRP (V12M, Q141K, A149P, R163K, Q166E, P269S, and S441N BCRP) after transfection of their cDNAs in plasmid vector to LLC-PK1 cells. Their expression levels and transport activities were determined using the membrane vesicles from HEK293 cells infected with the recombinant adenoviruses containing these kinds of BCRP cDNAs.

Results. Wild type and six different SNP variants of BCRP other than S441N BCRP were expressed on the apical membrane, whereas S441N BCRP showed intracellular localization. The expression levels of Q141K and S441N BCRP proteins were significantly lower compared with the wild type and the other five variants. Furthermore, the transport activity of E_1S, DHEAS, MTX, and PAH normalized by the expression level of BCRP protein was almost the same for the wild type, V12M, Q141K, A149P, R163K, Q166E, and P269S BCRP.

Conclusions. These results suggest that Q141K SNPs may associate with a lower expression level, and S441N SNPs may affect both the expression level and cellular localization. It is possible that subjects with these polymorphisms may have lower expression level of BCRP protein and, consequently, a reduced ability to export these substrates.

KEY WORDS: adenovirus; BCRP/ABCG2; interindividual difference; SNPs.

INTRODUCTION

ABCG2, also referred to as breast cancer resistance protein (BCRP), mitoxantrone resistance-associated protein (MXR), and placenta-specific ATP-binding cassette transporter (ABCP), is a member of the ATP-binding cassette (ABC) transmembrane transporter family (1–3). BCRP mRNA encodes a 72.6 kDa membrane protein composed of 655 amino acids (1,3,4). It has a single ATP binding domain at the amino terminus (at amino acid 61-270) followed by six transmembrane domains (at amino acids 394-416, 428-450, 478-499, 506-528, 533-555 and 629-651) (1,5). BCRP may form a homodimer to become functionally active (6). In BCRP-expressing cells, the intracellular concentration of substrate anticancer drugs is reduced, suggesting its protective role against drug toxicity (7). In normal human tissues, BCRP is expressed on the apical membrane of enterocytes, trophoblast cells in the placenta, the bile canalicular membrane of hepatocytes, and the apical membrane of lactiferous ducts in the mammary gland (8). Current evidence indicates that BCRP could contribute to the disposition of some substrates (9,10). Moreover, it was recently shown that BCRP also transports some endogenous compounds such as sulfate conjugates (11). It is also reported that some mutations in the open reading frame of BCRP are associated with resistance to some anticancer drugs. For example, an amino acid mutation at position 482 affects the resistance to adriamycin and methotrexate (12,13). Therefore, it is possible that certain kinds of single nucleotide polymorphisms (SNPs) of BCRP may alter its function and, consequently, affect the disposition of substrate drugs.

To date, some pieces of information about BCRP SNPs have been reported. Recently, the SNPs of BCRP in 100 healthy Japanese subjects have been analyzed in 84 cell lines established from clinically dissected human tumors and also in 60 Japanese individuals who were given irinotecan, an anticancer drug, for the treatment of various types of cancer (14). On analyzing the specimens from the 100 Japanese volunteers, 7 kinds of SNPs were identified for the BCRP gene: G34A (V12M), C376T (Q376Stop), C421A (Q141K), G1098A (E366E), G1322A (S441N), T1465C (F489L), and C1515- (AFFVM505-509ASSL Stop). The allele frequencies of these SNPs are 18, 1, 36, 1, 0.5, 0.5, and 0.5%, respectively. In the 84 cell lines, 7 kinds of SNPs were identified and their frequency for G34A (V12M), C376T (Q126Stop), C421A (Q141K), G445C (A149P), G488A (R163K), C805T (P269S), and G1098A (E366E) are 22, 3, 29, 1, 0.6, 0.6 and 2%, respectively. In the present study, we focused on the 7 SNPs, 6 of which were found in Japanese samples and cell samples, and 1 was reported in the NCBI database (rs1061017). We constructed expression systems for the wild type and SNPs variants of BCRP (V12M, Q141K, A149P, R163K, Q166E, P269S, S441N BCRP) and examined whether these SNPs variants of BCRP alter its localization, expression level, and transport activity.

MATERIALS AND METHODS

Materials

[^{3}H]Estrone-3-sulfate (E_1S; 46 Ci/mmol), [^{3}H]dehydroepiandrosterone sulfate (DHEAS; 79.1 Ci/mmol), and [^{3}H]*p*-aminohippuric acid (PAH; 4.51 Ci/mmol) were purchased from PerkinElmer Life Science, Inc. (Boston, MA, USA). [^{3}H]Methotrexate (29 Ci/mmol) was purchased from Ameri-

[1] School of Pharmaceutical Sciences, The University of Tokyo, Hongo, Bunkyo-ku, Tokyo 113-0033, Japan.
[2] Department of Pharmacy, Tokyo University Hospital, The University of Tokyo, Hongo, Bunkyo-ku, Tokyo 113-0033, Japan.
[3] National Institute of Health Sciences, Kamiyoga, Setagaya-ku, Tokyo 158-8501, Japan.
[4] School of Pharmaceutical Sciences, Kyushu University, Maidashi, Higashi-ku, Fukuoka 812-8582, Japan.
[5] Department of Hospital Pharmacy, Faculty of Medicine, Tottori University, Yonago, Tottori, 683-8504, Japan.
[6] To whom correspondence should be addressed. (e-mail: sugiyama@mol.f.u-tokyo.ac.jp)

ABBREVIATIONS: ABC transporter, ATP-binding cassette transmembrane transporter; Ad, adenovirus; BCRP, breast cancer resistance protein; DHEAS, dehydroepiandrosterone sulfate; E_1S, estrone 3-sulfate; ER, endoplasmic reticulum; K_m, Michaelis constant; MOI, multiplicity of infection; MTX, methotrexate; PAH, *p*-aminohippurate; SNPs, single nucleotide polymorphisms; V_{max}, maximum transport velocity.

can Radiolabeled Chemicals, INC. (St. Louis, MO, USA). Unlabeled E_1S, DHEAS, methotrexate, PAH, and ATP, creatine phosphate, and creatine phosphokinase were purchased from Sigma Chemical (St. Louis, MO, USA). All other chemicals used were commercially available and of reagent grade.

LLC-PK1 and HEK293 cells were cultured in Medium 199 (GIBCO BRL, Gaithersburg, MD, USA) and Dulbecco's modified Eagle's medium (GIBCO BRL), respectively, after addition of 10% fetal bovine serum, and penicillin (100 U/ml) and streptomycin (100 mg/ml).

Construction of BCRP-Containing Expression Vectors and Recombinant Adenovirus

Wild-type BCRP cDNA was purchased from Invitrogen Corp. (Carlsbad, CA, USA) (no. H24176). The complete BCRP cDNA was amplified with the primers containing NheI site and Kozak sequence attached at the 5'-end and that with the ApaI site at the 3'-end by PCR, and then was inserted into pcDNA3.1 vector plasmid, resulting in wt BCRP/pcDNA3.1. Using site-directed mutagenesis, SNP variants of BCRP (V12M, Q141K, A149P, R163K, Q166E, P269S and S441N BCRP) were constructed on pcDNA3.1 vector (SNPs type BCRP/pcDNA3.1). V12M BCRP was amplified with 5'-GTCGAAGTTTTTATCCCAATGTCACAAGGAAA-CACCAATGGC-3' and '-GCCATTGGTGTTTCCTTGT-GACATTGGGATAAAAACTTCGAC-3'. Q141K BCRP was amplified with 5'-CGGTGAGAGAAAACT-TAAAGTTCTCAGCAG-3' and '-GCTGCTGAGAACTT-TAAGTTTTCTCTCACCG-3'. A149P BCRP was amplified with 5'-GCAGCTCTTCGGCTTCCAACAACTATGACG-3' and '-CGTCATAGTTGTTGGAAGCCGAAGAGC-TGC-3'. R163K BCRP was amplified with 5'-CGAACGGATTAACAAGGTCATTCAAGAG-3' and 5'-CTCTTGAATGACCTTGTTAATCCGTTCG-3'. Q166E BCRP was amplified with 5'-GATTAACAGGGTCATT-GAAGAGTTAGGTCT-3' and 5'-CCAGACCTA-ACTCTTCAATGACCCTGTTAA-3'. P269S BCRP was amplified with 5'-GACTTATGTTCCACGGGTCTGCT-CAGGAGGCCTTGGG-3' and 5'-CCCAAGGCCTCCT-GAGCAGACCCGTGGAACATAAGTC-3'. S441N BCRP was amplified with 5'-CCAACCAGTGTTTCAGCAAT-GTTTCAGCCGTGGAACTC-3' and 5'-GAGTTCCACG-GCTGAAACATTGCTGAAACACTGGTTGG-3'. From these pcDNA3.1 vectors, BCRP cDNA was subcloned into the NheI and ApaI sites of the pShuttle plasmid vector, transferred into Adeno-XTM Viral DNA using the Adeno-X Expression System (BD Biosciences, Palo Alto, CA, USA), resulting in pAd-wt BCRP. To produce recombinant adenovirus, pAd-wt BCRP was digested with PacI, and transfected to HEK293 cells by FuGENE6 (Roche Diagnostics Corporation, Indianapolis, IN, USA) according to the manufacturer's instructions. For SNPs type BCRPs, viruses were prepared in the same way, resulting in the production of pAd-SNPs BCRP (pAd-V12M, Q141K, A149P, R163K, Q166E, P269S, and S441N BCRP). Recombinant viruses prepared as described previously (Ad-wt BCRP and Ad-SNPs type BCRP) (15) were purified by CsCl gradient centrifugation, dialyzed with a solution containing 10 mM Tris (pH 7.5), 1 mM $MgCl_2$, and 10% glycerol, and stored in aliquots at -80°C. Then, the resulting virus titer was determined as described previously (16).

Immunohistochemical Staining

For immunohistochemical staining, LLC-PK1 cells transfected with wild-type BCRP or SNPs type BCRP in pcDNA3.1 vector were plated at a density of 5×10^5 cells in 12-well dishes, 72 h prior to the experiments. After fixation with 4% (w/v) paraformaldehyde for 10 min and permeabilization in 1% TritonX-100 in PBS for 10 min, cells were incubated with the monoclonal antibody against BCRP (BXP-21) (Kamiya Biomedical Company, Seattle, WA, USA) for 1 h at room temperature. Then, cells were washed three times with PBS and incubated with Goat anti-mouse IgG Alexa 488 (Molecular Probes, Inc., Eugene, OR, USA) diluted 250-fold in PBS for 1 h at room temperature, and mounted in VECTASHIELD Mounitng Medium (Vector Laboratories, Burlingame, CA, USA). The localization of BCRP protein was visualized by confocal lazer microscopy (Zeiss LSM-510; Carl Zeiss Inc., Thornwood, NY, USA).

Preparation of Membrane Vesicles

To prepare membrane vesicles, HEK293 cells were plated at a density of 2×10^6 cells per 15 cm dish. After 72 h, cells were infected with recombinant adenoviruses containing the wild-type and SNPs type BCRP at 2×10^7 pfu per plate. As a negative control, cells were infected with the virus containing GFP cDNA (pAd-GFP). Cells were harvested at 48 h after infection and then the membrane vesicles were isolated using a standard method described previously in detail (17). Briefly, cells were diluted 40-fold with hypotonic buffer (1 mM Tris-HCl, 0.1 mM EDTA, pH 7.4, at 4°C) and stirred gently for 1 h on ice in the presence of 2 mM phenylmethylsulfonyl fluoride, 5 μg/ml leupeptin, 1 μg/ml pepstatin, and 5 μg/ml aprotinin. The cell lysate was centrifuged at 100,000 × *g* for 30 min at 4°C and the resulting pellet was suspended in 10 ml isotonic TS buffer (10 mM Tris-HCl, 250 mM sucrose, pH 7.4 at 4°C) and homogenized in a Dounce B homogenizer (glass/glass, tight pestle, 30 strokes). The crude membrane fraction was layered on top of a 38% (w/v) sucrose solution in 5 mM Tris-HEPES, pH 7.4 at 4°C, and centrifuged in a Beckman SW41 rotor centrifuge at 280,000 × *g* for 45 min at 4°C. The turbid layer at the interface was collected, diluted to 23 ml with TS buffer, and centrifuged at 100,000 × *g* for 30 min at 4°C. The resulting pellet was suspended in 400 μl TS buffer. Vesicles were formed by passing the suspension 30 times through a 27-gauge needle using a syringe. The membrane vesicles were finally frozen in liquid nitrogen and stored at -80°C until required. Protein concentrations were determined by the Lowry method.

Western Blot Analysis

For the Western blot analysis, membrane vesicles were dissolved in 3 x SDS sample buffer (New England BioLabs, Beverly, MA, USA), and separated on a 10% SDS-polyacrylamide gel electrophoresis plate with a 4.4% stacking gel. The molecular weight was determined using a prestained protein marker (New England BioLabs). Proteins were transferred electrophoretically to a polyvinylidene diflouride membrane (Pall, East Hills, NY, USA) using a blotter (Bio-Rad Laboratories, Richmond, CA, USA) at 15 V for 1 h The membrane was blocked with PBS containing 5% skimmed milk for 1 h at room temperature. After blocking, the membrane was incubated for 1 h at room temperature in BXP-21

(Kamiya Biomedical Company, Seattle, WA, USA) diluted 100-fold with 5% skimmed milk. Then, the membrane was washed with PBS containing 0.1% Tween-20 and allowed to bind to Alexa Fluor 680 goat anti-mouse IgG (Molecular Probes, Inc. Eugene, OR, USA) which was diluted 5,000-fold with skimmed milk for 1 h to detect BCRP. Subsequently, the fluorescence was measured in a densitometer (Odyssey, ALOKA, Tokyo, Japan). The protein expression levels of each SNPs variant of BCRP were determined by analyzing the band density associated with three different applied amount of the membrane vesicles on the Western blot analysis.

Vesicle Transport Assays

The uptake study of [^{3}H]E_1S, [^{3}H]DHEAS, [^{3}H]MTX, [^{3}H]PAH was performed as reported previously (18). Briefly, the transport medium (10 mM Tris, 250 mM sucrose and 10 mM $MgCl_2$, pH 7.4) contained the ligands, 5 mM ATP and an ATP-regenerating system (10 mM creatine phosphate and 100 mg/ l creatine phosphokinase). An aliquot of transport medium (15 μl) was mixed rapidly with the vesicle suspension (2 μg protein for [^{3}H] E_1S and 10 μg protein for others in 5 μl). The transport reaction was stopped by the addition of 1 ml ice-cold buffer containing 250 mM sucrose, 0.1 M NaCl and 10 mM Tris-HCl (pH 7.4). 900 μl of the stopped reaction mixture was passed through a 0.45 μm HA filter (Millipore Corp., Bedford, MA, USA), and then washed twice with 5 ml stop solution. The radioactivity retained on the filter was measured in a liquid scintillation counter (LS 6000SE, Beckman Instruments, Fullerton, CA, USA) after the addition of scintillation cocktail (Clear-sol I, Nacalai Tesque, Tokyo, Japan). The amount of ligand taken up into vesicles was normalized in terms of the amount of membrane protein. The uptake activity was defined as the amount of ligand divided by the ligand concentration in the medium. The ATP-dependent uptake of ligands was calculated by subtracting the ligand uptake in the absence of ATP from that in its presence.

RESULTS

Localization of Human BCRP in LLC-PK1 Cells

The localization of human BCRP was determined by immunohistochemical staining. Monoclonal antibody against human BCRP (BXP-21) detected a high fluorescence signal at the apical membrane of LLC-PK1 cells after transfection of the wild type BCRP/pc DNA3.1 (Fig. 1). No specific fluorescence signal was observed at the apical membrane or in the cytoplasm after transfection of pcDNA3.1 plasmid vector (data not shown). We also analyzed the cellular localization of BCRP variants. In our experimental system, except for one SNP variant of BCRP (S441N BCRP/pcDNA3.1), all variants showed the same localization as the wild-type BCRP, at the apical membrane of LLC-PK1 cells (Fig. 1). S441N BCRP was expressed intracellularly (Fig. 1).

Expression Level of Human BCRP in HEK293 Cells Using Recombinant Adenoviruses

The expression level of BCRP in the membrane fraction isolated from the BCRP-expressing HEK293 cells was determined by Western blot analysis using an anti-human BCRP monoclonal antibody (BXP-21). As previously reported, BCRP was detected at an approximate molecular weight of 72 kDa (Fig. 2). In contrast, in the membrane vesicles from the Ad-GFP infected cells, no BCRP was detected (Fig. 2). The expression levels of wild-type BCRP and variants were estimated from the band density. Except for two BCRP variants (Q141K and S441N BCRP), the expression levels of each BCRP SNPs were approximately the same as that of the wild-type BCRP (Fig. 2). The expression level of Q141K BCRP was approximately 30–40% of the wild-type BCRP, whereas that of S441N BCRP was much lower, and could not be determined with any accuracy (Fig. 2).

Transport Activity of BCRP

Because we previously reported that [^{3}H]E_1S is taken up into BCRP-expressing membrane vesicles in an ATP-

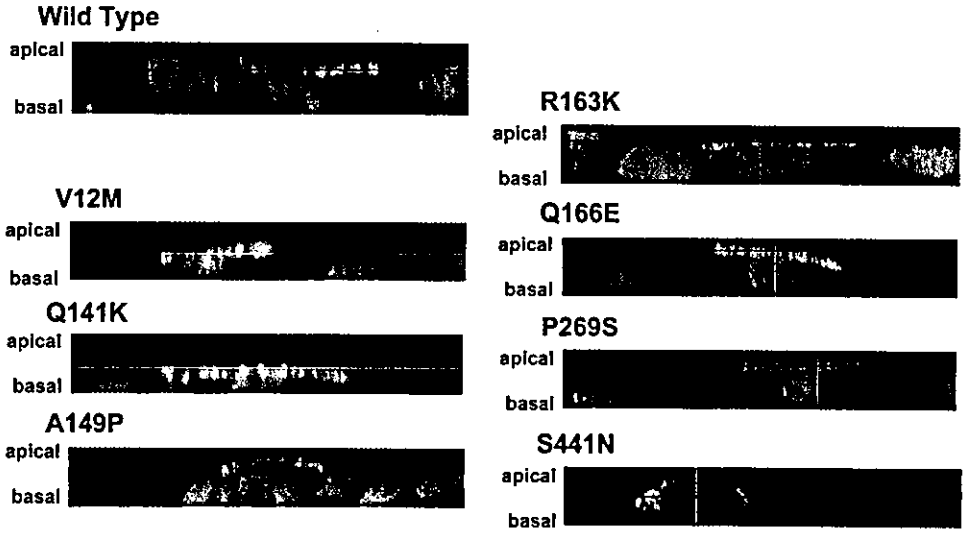

Fig. 1. Localization of BCRP in LLC-PK1 cells. The immunolocalization of BCRP molecules in the LLC-PK1 cells transfected with BCRP cDNA was determined using monoclonal antibody against BCRP (green). Nuclei were stained with PI (red). Figures show the Z-sectioning images, top side of the figure shows the apical membrane, and bottom side is the basal membrane.

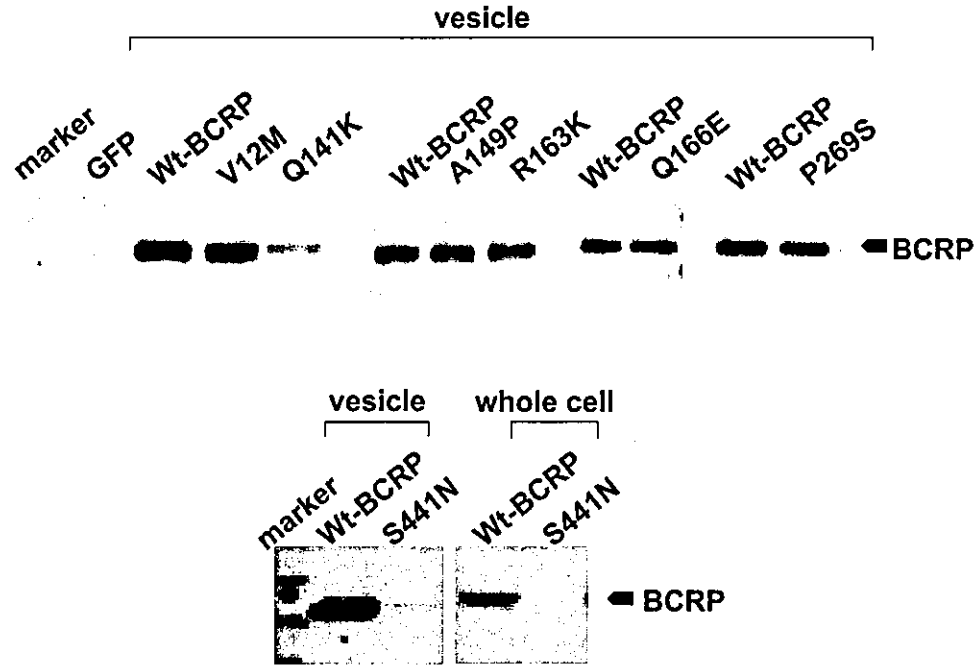

Fig. 2. Expression level of BCRP in membrane vesicles. The expression level of the wild type and SNPs variants of BCRP proteins was determined in the isolated membrane vesicles from HEK293 cells infected with recombinant adenovirus using Western blot analysis. The expression levels of wild type and S441N SNPs BCRP were also determined also in whole cell lysates.

dependent manner (11), the effect of SNPs on the BCRP-mediated transport of [^{3}H]E_1S was examined. In the current study, we used the same batch of transfected cells for measurement of the expression level and transport activity. Ad-wt BCRP expressing membrane vesicles transported [^{3}H]E_1S up to approximately 0.5 nmol min^{-1} mg^{-1} membrane protein, whereas no uptake of [^{3}H]E_1S was observed by the membrane vesicles from Ad-GFP infected cells. Because the amount of [^{3}H]E_1S molecules taken up by 2 μg membrane vesicles at 1 min (1 pmol) is approximately 1/10 of that in the incubation medium (10 pmol), [^{3}H]E_1S molecules were not depleted from the incubation medium. Based on this consideration, it is possible for us to determine the initial uptake velocity from 1 min data. Indeed, we could find that the time profile for the BCRP-mediated uptake of [^{3}H]E_1S was linear up to 2 min.

Except for two SNP variants of BCRP (Q141K and S441N BCRP), the ATP-dependent uptakes per mg membrane protein of SNP variants (V12M, A149P, R163K, Q166E, P269S BCRP) were similar to that of the wild-type BCRP (Fig. 3a). The uptake activity of Q141K BCRP per mg membrane protein was approximately 30–40% of the wild-type BCRP, and that of S441N was almost the same as that of the GFP-infected control cells. These uptake activities were inhibited by the excess amount of E_1S, 100 μM (Fig. 3a).

Then, in order to compare the intrinsic transport activity of the wild-type and SNP variants of BCRP, the uptake determined per mg membrane protein (Fig. 3a) was normalized relative to the expression levels estimated by Western blot analysis (Fig. 2), except for S441N BCRP the expression level of which was extremely low (Fig. 2). As shown in Fig. 3b, the transport activity of other SNP variants of BCRP (V12M, Q141K, A149P, R163K, Q166E, and P269S BCRP) was almost identical to that of the wild-type BCRP.

As far as V12M and Q141K BCRP were concerned, these have a high allele frequency in Japanese and we determined the kinetic parameters for the transport of [^{3}H]E_1S. As shown in Fig. 4, the ATP-dependent uptake of [^{3}H]E_1S was saturable, and the K_m values were 11.6 ± 4.79, 9.07 ± 1.52, and 14.0 ± 7.27 μM, and the V_{max} values were 13.3 ± 3.3, 13.5 ± 1.29, and 4.57 ± 1.58 nmol min^{-1} mg^{-1} protein, for the wild type, V12M, and Q141K BCRP, respectively. In addition to [^{3}H]E_1S, the transport of other BCRP substrates was examined. As previously reported, ATP-dependent uptake of [^{3}H]methotrexate and [^{3}H]DHEAS was observed. The absolute values of their transport activity were about at 7.5 pmol 2 min^{-1} mg^{-1} mebrane protein and 150 pmol 2 min^{-1} mg^{-1} membrane protein, whereas GFP-expressing membrane vesicles tranport them at about 0.5 pmol 2 min^{-1} mg^{-1} membrane protein and 25 pmol 2 min^{-1} mg^{-1} membrane protein, respectively. Moreover, BCRP-mediated transport of [^{3}H]PAH was also detectable, and the activity of this was 10 pmol 2 min^{-1} mg^{-1} membrane protein, whereas GFP-expressing membrane vesicles tranport them at about 0.5 pmol 2 min^{-1} mg^{-1} membrane protein. Figure 5a shows the ATP-dependent uptake of DHEAS, PAH, and MTX per mg membrane protein for the wild-type and SNPs BCRP (V12M, Q141K, A149P, R163K, Q166E, P269S, and S441N BCRP). Although Q141K BCRP exhibited a lower activity than wild type BCRP, no significant transport was observed for S441N BCRP (Fig. 5a). Figure 5b shows the intrinsic transport activities normalized by the expression levels of BCRP protein. There was no significant difference between wild type BCRP and SNPs variants.

DISCUSSION

In the current study, we analyzed the function of BCRP SNPs in terms of their localization, expression level, and